1959

Air flow analysis of grain ventilation ducts

Gene Clere Shove
Iowa State University

AIR FLOW ANALYSIS OF GRAIN VENTILATION DUCTS

by

Gene Clere Shove

A Dissertation Submitted to the

Graduate Faculty in Partial Fulfillment of

The Requirements for the Degree of

DOCTOR OF PHILOSOPHY

Major Subjects: Agricultural Engineering
Theoretical and Applied Mechanics

Approved:

Signature was redacted for privacy.

Signature was redacted for privacy.

In Charge of Major Work

Signature was redacted for privacy.

Signature was redacted for privacy.

Heads of Major Departments

Signature was redacted for privacy.

Dean of Graduate College

Iowa State College

Ames, Iowa

1959

TABLE OF CONTENTS

	Page
DEFINITION OF SYMBOLS	1
INTRODUCTION	4
OBJECTIVE	6
REVIEW OF LITERATURE	7
ANALYSIS OF STATIC PRESSURE CHANGE IN A PERFORATED DUCT	38
EQUIPMENT AND EXPERIMENTAL PROCEDURE	45
RESULTS - SUCTION SYSTEM	53
RESULTS - PRESSURE SYSTEM	62
DISCUSSION	66
APPLICATION OF RESULTS	68
SUMMARY	79
CONCLUSIONS	81
LITERATURE CITED	82
ACKNOWLEDGMENTS	85
APPENDIX A: METHOD OF CALIBRATING PERFORATED METAL SHEETS USED FOR AIR FLOW MEASUREMENT	86
APPENDIX B: DETERMINATION OF THE FRICTION HEAD LOSS FOR THE TEST DUCT	88
APPENDIX C: AIR FLOW CALIBRATION OF THE PERFORATIONS IN THE TEST DUCT WALL	91
APPENDIX D: ORIGINAL AND CALCULATED DATA	95

DEFINITION OF SYMBOLS

The definitions of symbols given in Table 1 will be used throughout this dissertation. Since different writers often use different symbols to define a given factor, some of the symbols in the review of literature have been changed to agree with Table 1 and some of the equations have been rearranged.

Table 1. Definition of symbols

Symbol	Definition	Units
A	Cross-sectional area of main conduit, duct, manifold, or pipe	sq ft
a	Cross-sectional area of branch conduit, duct, or pipe	sq ft
b	Slot width	ft
C	Ratio of the velocity head of the fluid about to leave through a branch take-off to the average velocity head in the main upstream of the take-off	----
C_d	Coefficient of discharge	----
D	Diameter of duct or pipe	ft
f	Friction factor defined by $h_f = f\frac{LV^2}{D2g}$	----
F	Force	lb
g	Acceleration of gravity	ft/sec^2

Table 1. (Continued)

Symbol	Definition	Units
H	Total energy head	ft
ΔH	Total head loss or gain term in Bernoulli equation	ft
h	Static pressure head	ft
h_f	Head differential in Darcy-Weisbach equation	ft
K	Constant applied to velocity head change	----
k	Fraction of the momentum change of the entering or leaving fluid produced by a pressure change in the main duct	----
k_1	Coefficient defined on page 17	----
k_2	Coefficient defined on page 16	----
L	Active length of main duct	ft
M	Constant equal to $\frac{K}{A^2 g}$	----
m	Mass	lb/ft sec^2
N	Constant equal to $\frac{f}{A^2 D2g}$	----
n	An exponent	----
P	Fluid pressure	lb/sq ft
Q	Rate of fluid flow in main duct	cu ft/sec
q	Rate of fluid flow in branch duct or discharge or intake per unit length of perforated main duct	cu ft/sec
r	Resistance constant in Equation 14	----

Table 1. (Continued)

Symbol	Definition	Units
t	Time	sec
u	Velocity component of V_b parallel to main duct	ft/sec
V	Velocity	ft/sec
v	Velocity component of V_b normal to main duct	ft/sec
w	Specific weight of fluid	lb/cu ft
x	Distance from dead end of main duct	ft
α	Branching angle or angle entering or leaving fluid makes with the main duct measured in a clockwise direction from the upstream side	----
ρ	Density	lb sec^2/ft^4
τ	Frictional force per unit area of duct wall	lb/sq ft

The following subscripts were used:

b	Branch cross section
d	Downstream cross section
i	Intake port or opening
j	Discharge port or opening
L	Head end of main duct
o	Dead end of main duct
p	Pressure system (static pressure above atmospheric)
s	Suction system (static pressure below atmospheric)
u	Upstream cross section.

INTRODUCTION

The use of mechanical ventilation for maintaining the quality of stored grain has become an important practice in the management of commercial grain storages. Mechanical ventilation also has been used to help maintain the quality of the large volume of surplus grain owned by the Federal government. During recent years grain ventilation has received considerable attention in "on-the-farm" storage since grain often is stored on the farm for extended periods under government price support loans.

Grain ventilation includes the movement of relatively small amounts of air through grain for the prevention of moisture migration, the movement of larger amounts of air for grain cooling, and the movement of maximum amounts of air for grain drying. The problem of air distribution in grain ventilation is to provide economically sufficient air flow through all parts of the grain. An equitable air distribution for ventilating grain can be obtained by the use of false floors under the grain; however, in storage buildings with large floor areas duct systems often are used. The usual practice is to employ ducts of uniform cross section having uniform air inlet openings along their length. Apparently there is no known reliable method for designing the ventilating ducts to insure uniform air flow throughout the grain.

The problem of selecting or designing a constant cross section ventilating duct can be divided into two phases: (1) prediction of the variation in the air intake or discharge along the length of the duct if the area of the intake or discharge openings is constant along the length of the duct and (2) design of the variation of the air-opening area to produce uniform air intake or discharge along the length of the duct. Since the air intake or discharge is related to the static pressure gradient in the duct, the problem of selecting or designing a ventilating duct requires prediction of the static pressure gradient.

In vertical storages where uniform floor collector ducts are relatively short in length compared with the depth of the grain, the pressure drop within the ducts will be small, causing only negligible nonuniformity of air flow. In flat storages equipped for ventilation with uniform longitudinal floor ducts, the length of the duct becomes long in comparison with the depth of the grain. Under these conditions there may be a considerable pressure drop in the ducts, and the air flow distribution along the length of the ducts may be entirely unsatisfactory.

OBJECTIVE

The objective of this study was to establish experimentally a relationship between the static pressure gradient and air flow in a perforated duct in order to analyze pressures and air flows in grain ventilating ducts and to provide a basis for grain ventilating duct design.

REVIEW OF LITERATURE

An experiment, described by Robinson et al. (31), performed in 1943 at Ames, Iowa, demonstrated that differences in temperatures occurring in stored grain held from summer or early fall through the following winter set up convection currents and vapor-pressure differences between various parts of the grain pile. These convection currents and vapor-pressure differences cause a slow exchange of moisture, referred to as moisture migration, from the warmest grain to that which is cool. Since the exposed surface of the grain pile is the first portion to cool as atmospheric temperatures begin to drop in late fall and early winter, an increase in grain moisture usually occurs at or near the top surface of the pile. The onset of warmer ambient temperatures in the spring and summer may be inducive to detrimental mold growth and/or insect activity in this region of high moisture. Considerable damage in the form of moldy, caked grain is often the result.

Various methods have been used in attempting to eliminate or control grain damage caused by moisture migration. Stirring and mixing the surface layers of the grain may reduce the seriousness of spoilage but does not correct the trouble. This procedure also requires considerable labor. Commercial grain storage operators often rely on the practice of "turning" the grain, that is, moving the grain

through air. Turning requires conveying equipment and extra storage space, and several turnings may be necessary to accomplish satisfactory results.

Another method of controlling moisture migration, referred to as grain aeration or grain cooling, is to move air through the grain by the use of motor-driven fans. These fans usually are operated as exhaust fans, pulling air through the grain. Johnson (21, p. 238) made the following comments on the practicality of aerating grain:

> The cooling of stored grain in relatively large-sized storage units, such as terminal elevators, by aeration is becoming recognized as an advantageous and economically feasible practice under many conditions commonly found in the operation of various types of grain-storage facilities. Such aeration systems provide a measure of temperature and moisture control which has a definite effect in limiting both insect and microfloral activity. In addition, aeration offers a means for minimizing temperature differences within the grain mass itself, thus preventing the moisture migration which leads to chemical deterioration of stored grain.

Holman (15, p. 1) has listed five purposes for the use of aeration systems in commercial storages:

1. Cooling stored grain to prevent or minimize mold growth and insect activity.
2. Equalizing temperatures in stored grain to prevent moisture from moving from warm to cooler grain.
3. Removing odors from stored grain.
4. Applying fumigants to stored grain.
5. Holding moist grain in storage for brief periods.

Considerable attention has been given to the determination of the power requirements and operational procedures for aeration systems. Holman (15, pp. 20-25) has compiled information for estimating the fan horsepower and static pressure requirements for aerating grain of various kinds. Theimer (36) has prepared a psychrometric chart for ventilated grain storage for determining the optimum atmospheric conditions for safe ventilation. However, little information is available on the design of the air distribution or collector duct. Rabe (30, p. 99) stated:

> To assure uniform air flow through the grain, the external collector area per foot of length, should be constant. Actually, this area should increase slightly in proportion to the pressure drop of the air within the collector and in a direction away from the fan. Unless the air velocities in the collector or aeration duct are excessive and the collector is very long, the pressure drop of the air within this enclosure may be neglected. It is evident that, for a given installation, the effective external surface of an aeration duct influences the amount of air circulated. The aeration rate decreases as this area is decreased.

Hall (12, pp. 144-147) stated:

> For low air flows such as used for cooling of grain in flat storages uniform air distribution has often been difficult to obtain where an open duct system cylindrically-shaped with at least 30 percent openings has been used. With a suction system the greatest quantity of air is moved through the grain next to the fan. The openings in the duct should be selected to throttle the air to provide uniform air flow throughout the length of the duct. Air flows are throttled by the duct if there is less than 7 percent openings. An ideal arrangement would consist of providing a duct with perhaps one percent openings at points of otherwise high air flows varying to perhaps 7 percent openings at the opposite end. The air velocity in the duct is usually from 1000 to 3000 ft per min. Data are needed

> but not now available relating air flow direction . . . and volume, openings in duct, and pressure drop through product to design air flow systems with uniform air distribution.

In general the experiments described in literature on the hydraulics of perforated pipe or intersecting junctions of pipes have been concerned with pressure systems. However, many writers have indicated the expressions for a pressure system can be applied, with only slight modification, to suction systems.

Apparently the earliest attempts to analyze the hydraulics of perforated pipe were made in connection with the washing of sand filters. One of the most common systems for distributing the wash water consisted of a header with perforated lateral pipes. The purpose of early experiments was to devise methods for designing these systems to provide a uniform distribution of the wash water.

Ellms (5) described some early experiments and set forth the following design limits that should not be exceeded if uniform distribution is desired: (1) the sum of the cross-sectional areas of the laterals should be at least twice the sum of the cross-sectional areas of the perforations in the laterals, (2) the cross-sectional area of the manifold or header should be 1.75 to 2.00 times the sum of the cross-sectional area of the laterals which it feeds, and (3) the ratio of the length of the lateral to its diameter should not exceed 60.

In a discussion of Ellms' article, Malishewsky (26) said the pressure

distribution in a filter system can be determined by assuming the loss of velocity head will be converted completely to static pressure head. In a later article Malishevsky (25) stated the velocity head would be recovered in laterals with orifices on both sides; however, in laterals with orifices on one side only the velocity head in the lateral would be recovered by only 40 to 50 percent.

Enger and Levy (6) developed a formula for pressure on a slot in a pipe by considering a long, narrow slot along the length of the pipe. They neglected friction and wrote a momentum equation for an elemental length of pipe as

$$\left[wA(h + dh) - wAh\right] dt = \frac{wVA}{g} dt \left[(V - dV) - V\right]$$

hence

$$dh = - \frac{V}{g} dV$$

$$\int dh = - \frac{1}{g} \int V \, dV$$

$$h = - \frac{V^2}{2g} + h_o \qquad (1)$$

where h_o is the static pressure at the dead end. When pipe friction is neglected, the pressure on any point of the slot, according to Equation 1, is equal to the static pressure head at the end of the slot minus the velocity head at the given point. This indicates the velocity head is converted completely to static pressure head.

Enger and Levy assumed the coefficient of discharge in the flow equation

$$q = C_d b\, dx \sqrt{2gh}$$

remains constant and derived the equation for pressure along the slot as

$$h = \frac{h_o}{2} \quad \text{vers} \left[\pi - \frac{2C_d b}{A} \quad x \right] . \tag{2}$$

Enger and Levy commented that the coefficient of discharge of the openings in a pipe actually decreases as the velocity in the pipe increases. From their data they derived the following empirical formula for the variation of the discharge coefficient:

$$C_d = \frac{h - \frac{V^2}{2g}}{h} \quad C_{do} \tag{3}$$

in which $V^2/2g$ is the velocity head of the water in the pipe approaching the opening and C_{do} is the coefficient of discharge of the opening at the dead end.

Enger and Levy tabulated the data for one set of experiments made on ten, 3/8-inch openings spaced 6 inches center to center in a 2-inch water pipe. The values for friction loss were determined experimentally by tests on the same type of 2-inch water pipe. The observed values of the pressure head agreed closely with those calculated by Equation 1;

however, their pressure range was only 3.22 feet of water at the inlet end to 3.38 feet of water at the dead end.

Kunz (23) attempted to derive analytically Enger and Levy's equation for the variation of the discharge coefficient. Apparently his derivation was based on the assumption the coefficient of discharge at a particular point is proportional to the static pressure head at that point. He did, however, derive an expression similar to Equation 2.

An oversimplified analysis of the loss of head in uniformly-tapped pipes was made by Gladding (11). He assumed uniform outlets evenly spaced along a main duct would each discharge the same quantity of fluid. Edwards (4) and Howland (19) pointed out that Gladding's assumption of uniform discharge was not possible and did not represent a close approximation of actual conditions except for a pipe having an extremely large cross-sectional area compared with the total outlet area.

The analyses of pressure losses at the junctions of intersecting pipes appear to have application to the hydraulics of perforated pipes. A perforated pipe can be envisioned as a main conduit with many branches. In a perforated pipe the length of each branch duct usually will be equal to the wall thickness of the pipe.

Stevens (35), in considering the theoretical energy losses in intersecting pipes, equated the change of pressure to the change of momentum. Stevens neglected friction and wrote an expression for

the pressure change for two intersecting pipes (Fig. 1) as

$$(P_u - P_d)A = \frac{wQ_d}{g} V_d - w\left[\frac{q_1}{g} V_{b1} \cos \alpha_1 + \frac{q_2}{g} V_{b2} \cos \alpha_2\right]$$

which upon substitution of $Q_d = AV_d$ and $q = aV_b$ becomes

$$\frac{P_u - P_d}{w} = 2 \frac{V_d^2}{2g} - 2 \frac{V_{b1}^2}{2g} \frac{a_1}{A} \cos \alpha_1 - 2 \frac{V_{b2}^2}{2g} \frac{a_2}{A} \cos \alpha_2. \quad (4)$$

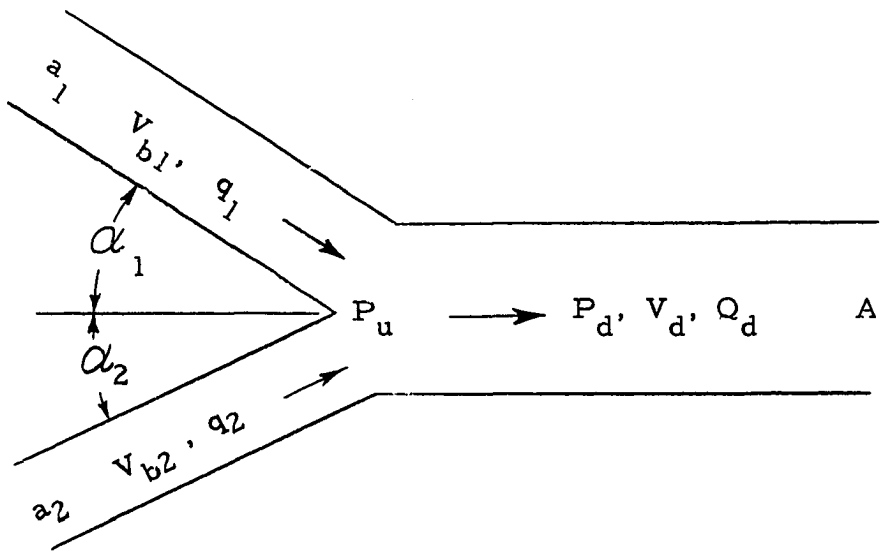

Fig. 1. Intersection of two branches with a main duct

Favre (7) considered the same momentum equation as Stevens and made a detailed and comprehensive analysis of combining flow.

He assumed negligible friction losses and derived the following expression for the change in static pressure at the junction of one branch with a main duct:

$$h_u - h_d = 2\left[\frac{V_d^2}{2g} - \frac{V_u^2}{2g}\right] - 2\,\frac{a}{A}\,\frac{V_b^2}{2g}\cos\alpha\,.$$

Favre then showed experimental work conducted at the Munich Hydraulic Institute on 45, 60, and 90 degree laterals was in agreement with his analysis. In summary he remarked his analysis applied particularly to combining flow because the fluid in the branch is directed into the main conduit at an angle nearly equal to the branch angle. The momentum of the entering fluid in the direction of the main flow can be represented by

$$-\frac{w}{g}\,q\,V_b\cos\alpha\,.$$

In the case of dividing flow, Favre stated the fluid leaves the main conduit without being compelled to follow any one direction. Therefore, the fluid leaving the main duct follows complicated laws that must be studied by experimentation.

During the course of this study, but prior to knowledge of Favre's article, an analysis of static pressure change in a perforated duct was developed as the analytical basis for the study. This analysis,

presented in the section following the review of literature, was found to be nearly identical with Favre's earlier analysis.

Oakey (29), reporting on a series of tests on hydraulic losses of short tubes in the sides of pipes, represented the losses by multiplying the upstream velocity by suitable coefficients. He began his derivation with the energy equation

$$Q_u w \left[\frac{V_u^2}{2g} + h_u\right] = Q_d w \left[\frac{V_d^2}{2g} + h_d\right] + qw \left[\frac{q}{Q_u} \quad \frac{V_u^2}{2g} + h_u\right]$$

which he simplified to

$$h_d - h_u = \left[3 \frac{q}{Q_u} - \left(\frac{q}{Q_u}\right)^2\right] \frac{V_u^2}{2g} . \qquad (5)$$

In the energy equation Oakey assumed the head under which the short tube discharged was equal to

$$\frac{q}{Q_u} \quad \frac{V_u^2}{2g} + h_u .$$

He called the change in pressure given by Equation 5 the theoretical rise in the hydraulic gradient between points upstream and downstream of the short-branch tube. The actual observed rise in the hydraulic gradient was represented by $k_2 \frac{V_u^2}{2g}$.

The difference between the theoretical rise and the actual rise in the hydraulic gradient is the lost head, which Oakey represented by

$$k_1 \frac{V_u^2}{2g} .$$

Oakey tabulated the k-values for four diameter ratios, D_b/D, 1 to 4.24, 1 to 2.82, 1 to 1.82, and 1 to 1.21. In general, as the flow ratio, q/Q_u, varied from 0.1 to 1.0, k_1 varied from about 0.1 to 1.3. The value of k_2 varied from about 0.2 to a peak of around 0.8 or 0.9 at $q/Q_u = 0.7$ and then decreased to about 0.7 at $q/Q_u = 1.0$.

Oakey also gave the following equation for determining the coefficient of discharge of the short-branch tube:

$$q = C_d a \sqrt{2g\left[\frac{q}{Q_u}\frac{V_u^2}{2g} + h_u\right]} . \qquad (6)$$

In a discussion of the manifold problem, Keller (22, p. 77) stated:

> There are only two important factors which determine the distribution of flow in and from manifolds; these are (1) inertia and (2) friction. The former corresponds to change of velocity head. In general, as the fluid flows along the manifold its longitudinal velocity decreases, due to part of the fluid volume being discharged laterally through the openings. Therefore the fluid in the manifold is being decelerated and, in accordance with Bernoulli's theorem, this tends to increase the fluid pressure. Friction, on the other hand, results in loss of pressure along the length. The relative magnitudes of the pressure regain due to deceleration and the pressure loss due to friction determine whether the pressure rises or falls from the inlet end to the closed or dead end of the manifold. In cases where the

cross section of the manifold can be varied, it is usually possible so to proportion the area along the length that the two opposing factors just balance and the pressure remains constant at all points, resulting in uniform discharge per unit length.

Keller began his mathematical analysis of manifold flow by writing the fundamental equation for pressure rise in the direction of flow in an inlet manifold (Fig. 2a) as

$$\frac{dP}{w} = - \frac{d(V^2)}{2g} + f \frac{dx}{D} \frac{V^2}{2g} . \qquad (7)$$

The first term on the right-hand side of Equation 7 is the deceleration term and is negative because an increase of pressure corresponds to a decrease of velocity. The second term on the right is the friction term; and although friction always causes a decrease of pressure in the direction of flow, the term is positive since x is measured from the dead end, that is, in a direction opposing flow.

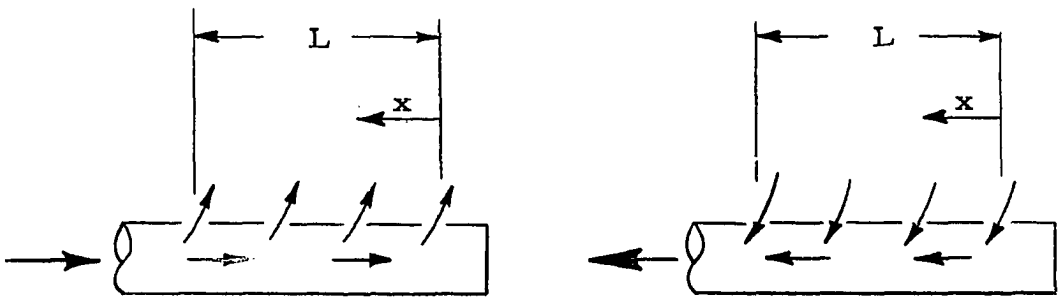

a. Inlet manifold b. Discharge manifold

Fig. 2. Sketch of manifold flow

Keller's expression for the pressure, P, at any distance, x, from the dead end in the inlet manifold (Fig. 2a) was

$$P = P_L + w \left[\frac{V_L^2 - V^2}{2g} \right] + \int_L^{(L-x)} f \frac{w}{D} \frac{V^2}{2g} dx. \qquad (8)$$

Since the manifold velocity, V, decreases linearly from its value, V_L, at the inlet end to zero at the dead end for uniform discharge, he substituted

$$V = V_L \frac{x}{L}$$

in Equation 8 and integrated to obtain

$$P = P_L + w \frac{V_L^2}{2g} \left[1 - \left(\frac{x}{L} \right)^2 \right] - \frac{fwL}{3D} \frac{V_L^2}{2g} \left[1 - \left(\frac{x}{L} \right)^3 \right]. \qquad (9)$$

In a similar manner Keller obtained the following expression for the pressure in a discharge manifold (Fig. 2b):

$$P = P_L + w \frac{V_L^2}{2g} \left[1 - \left(\frac{x}{L} \right)^2 \right] + \frac{fwL}{3D} \frac{V_L^2}{2g} \left[1 - \left(\frac{x}{L} \right)^3 \right]. \qquad (10)$$

In the discharge manifold, inertia and friction act in the same sense, both causing a decrease of pressure in the direction of flow.

Although Keller's Equations 9 and 10 appear more complicated than Enger and Levy's Equation 1, they are basically the same since

Keller's defining equation, Equation 7, states the change in velocity head is converted to pressure head. Keller, however, did include a friction term.

Keller also derived the following second-order differential equation for the velocity in a manifold of constant cross section with a uniform slot width or uniform distribution of holes:

$$\left[\frac{A}{C_d b}\right]^2 \frac{d^2V}{dx^2} = -V + \frac{f}{2D} \frac{V^2}{dV/dx} . \qquad (11)$$

He stated no solution had been found for this equation and used a point-by-point numerical method to obtain the velocity distribution.

In further discussion of manifold flow, Keller used two dimensionless ratios to define a manifold, namely, the

$$\frac{L}{D} \text{ ratio} = \frac{\text{active length of manifold}}{\text{diameter of manifold}}$$

and the

$$\text{area ratio} = \frac{\text{sum of areas of all discharge openings}}{\text{cross-sectional area of manifold}} .$$

Keller noted that manufacturers of pipe burners ordinarily state if the area ratio does not exceed unity, the distribution of gas discharge or the height of the flames will be practically uniform along the length of the burner pipe. He pointed out, however, that the above statement

does not take into consideration the effect of variation of the length/diameter ratio; and for L/D = 70, the friction practically cancels the deceleration regain. Keller showed that with an area ratio of unity and L/D ratios smaller or larger than 70, the discharge will not be uniform; and with an area ratio of 2 or greater, uniformity of discharge cannot be obtained regardless of the L/D ratio. Two cases from his own practice were cited in which the design of manifolds to yield uniform distribution based upon his analysis proved satisfactory.

Dow (3), in commenting on Keller's analysis, pointed out Keller failed to recognize the variation of the Reynolds number and the corresponding variation of the friction factor with distance along the manifold length. Consequently, Dow maintained the variation of the discharge is not a unique function of the L/D and area ratios but also depends on the rate of total flow. He demonstrated the variation of the discharge may be altered for any constant diameter, constant discharge-opening pipe by varying the total flow rate.

Dow used the same fundamental equations as Keller, stated for uniform distribution of discharge the static pressure must remain constant along the entire length of the manifold, and developed expressions for the variation in the diameter or hydraulic radius for an inlet manifold (Fig. 2a). He verified his results by placing tapered inserts in pipe burners and observing the resultant flame heights.

In 1935 Howland (18) discussed the apparent gain in total head that may be observed in a straight-flowing stream when a side stream separates from it. Howland (18, pp. 14-15) wrote:

> . . . if the Bernoulli equation is written . . . the so-called head loss term that must be introduced on the right side of the equation in order to balance it will, in general, be found to be negative for ratios of side flow to main flow of less than 1 to 2. In other words, a gain in head is observed.

He offered the following explanation of the apparent gain in head:

> . . . the branch scoops off the relatively slow-moving edge layers of water, leaving the fast-moving and therefore high-energy containing central core of water to flow past the take-off. The result is that the water continuing past the take-off has a higher average unit energy content, or head, than the complete stream approaching the take-off.

Based on these assumptions, Howland wrote an energy equation by ascribing a smaller velocity head to the fluid upstream about to leave through the take-off than the average velocity head at this section. He called the ratio of the velocity head of the fluid about to leave to the computed average velocity head "C" and wrote the following energy equation:

$$w Q_u \left[\frac{V_u^2}{2g} + h_u\right] = w Q_d \left[\frac{V_d^2}{2g} + h_d + \frac{(V_u - V_d)^2}{2g}\right] + wq \left[C \frac{V_u^2}{2g} + h_u\right]. \quad (12)$$

In this equation Howland assumed there was a loss of head in the straight-flowing stream equal to that in a sudden enlargement as given by the Carnot-Borda expression, $(V_u - V_d)^2/2g$.

Howland used Equation 12 and the results of his tests and tests performed at the Munich Hydraulic Institute to compute values of C and presented the results in graphic form. He drew some general conclusions regarding the value of C but did not derive any analytical expression which would permit the use of Equation 12 in the general case.

In a later paper Howland (17) based his design of a perforated pipe for uniformity of discharge on Enger and Levy's simple Bernoulli equation. He wrote the following equation for the static pressure at any point:

$$h = \frac{P}{w} = \frac{P_o}{w} - \frac{V_L^2}{2g}\left[\left(\frac{x}{L}\right)^2 - \frac{fL}{3D}\left(\frac{x}{L}\right)^3\right] \quad . \quad (13)$$

Equation 13 can be shown to be identical to Equation 9 presented by Keller.

Howland commented on the fact the coefficient of discharge for the perforations varied with the velocity in the pipe and the variation was much more pronounced in submerged discharge than in free discharge. In his computations Howland used values of the coefficient of discharge, C_d, obtained from experiments on the orifices in the

test pipe.

Howland did not state what fluid was used in his experimental work but described the pipe as a 16 foot long, 1.606-inch diameter, copper pipe perforated with 18 holes of 3/8-inch diameter. His tests compared the observed discharge of each hole with the discharge predicted by the flow equation:

$$q = C_d \; a\sqrt{2gH} \; .$$

Holdsworth et al. (14) presented an analysis of a leaky duct system by assuming the relationship between pressure gradient and flow rate in a leakless duct expressed by

$$\frac{dP}{dx} = r Q^n \qquad (14)$$

will be true also for a leaking duct. In a leaking duct the flow rate, Q, in Equation 14 will vary along the duct in a manner dependent on the nature of the leakage. Pressure regain or loss caused by the change in flow rate was conveniently neglected in Equation 14. Since their analysis applied to small leakage occurring at the seams and joints in air ducts, the neglect of any pressure change caused by the change in flow rate was apparently a reasonable simplification. However, in perforated ducts where there usually is a considerable

change in flow rate along the duct, this simplification cannot be applied.

Gilman (8, 9, 10) pointed out because of the innumerable possible combinations of different sizes and shapes of transitions which could be located at varying distances relative to each other, research usually had been restricted to a single transition under ideal conditions. The task of deciding what adjustment, if any, should be applied to the published data to suit a particular problem had been left to the engineer. Gilman said the closer together two transitions are located, the greater will be the deviation between the actual energy loss of the downstream transition and the value as predicted from data appearing in the literature.

For the straight-through flow in a dividing flow system Gilman used a single curve to represent the results of experimental work performed at the Munich Hydraulic Institute. Gilman wrote the following equation which closely approximated the curve representing the Munich tests:

$$ {}_{u}H_{d} = 0.35 \frac{(V_u - V_d)^2}{2g} . \qquad (15) $$

For the flow of air in ducts Gilman gave the following expression, which he credited to Carrier (2, p. 254):

$$ {}_{u}H_{d} = 0.5 \frac{V_u^2 - V_d^2}{2g} . \qquad (16) $$

In Equations 15 and 16 the total head loss, ${}_{u}H_{d}$, was considered to be concentrated at the section where the branch joins the main pipe, i.e., the losses are expressed on a "no length" basis. If a finite length of section is considered, the friction loss in the pipe section between u and d must be included.

In a discussion of the effect of the angle which the branch makes with the main duct, Gilman considered a main pipe having a small aperture from which a small stream issued at some angle α. Gilman assumed constant energy along the main stream and stated the angle α is determined by the flow conditions and the velocity ratio will be given by

$$\frac{V_b}{V_u} = \frac{1}{\cos \alpha} \quad . \tag{17}$$

Gilman defined the angle α in Equation 17 as the "natural" angle of discharge associated with a given velocity ratio. When this natural angle coincides with the angle of the branch duct, a point of minimum loss in the branch should be expected. Since Equation 17 is based on no velocity change in the main duct, he pointed out the minimum loss will occur at an angle greater than calculated by Equation 17 when there is an appreciable velocity change in the main duct. From a practical consideration Gilman stated one possible way of handling the same flow rate in each branch of the same size and length is to vary the

branching angle.

In concluding comments concerning divided flow elements, Gilman (10, p. 110) stated:

> The dissipation of mechanical energy (pressure loss) in nearly every through-flow type of duct element can be expressed in terms of the velocity head and a loss coefficient which depends on the geometry of the element and the conditions of the approaching flow.
>
> The pressure loss in a divided-flow element depends not only on the geometry of the element and the conditions of the approaching flow but also on the ratio of the volume rate diverted into the branch to that approaching the junction. The behavior of the loss curves for such elements can, however, be explained in a rational manner.

Allen and Albinson (1) suggested a step-by-step method for determining the variation in discharge port area for uniform discharge from each port of a manifold for a canal lock. Their analysis was based on a series of energy equations written for the fluid path through each port. Allen and Albinson's experimental work confirmed the step-by-step method of design. They also noted this method enabled the correct sizes of the ports to be estimated irrespective of the effective head.

Soucek and Zelnick (34, p. 1360), in their theoretical discussion of discharge ports in canal lock manifolds, considered the rate of change of momentum from points upstream and downstream of a port as

$$w \frac{Q_d}{g} (V_u - V_d) + w \frac{q}{g} V_u .$$

Soucek and Zelnick stated:

> The forces producing this effect are the pressure rise in the conduit and the resultant of unbalanced pressures within the port. The latter force is unknown and undeterminable in any practical manner except as a residual.

They assumed the unbalanced force is intimately related to the momentum change of q and allowed for its effect by modifying the momentum term, $w \frac{q}{g} V_u$. They considered k_j as the fraction of the momentum change of q which is produced by a pressure rise in the conduit and $1 - k_j$ as the fraction produced by the unbalanced pressure within the port.

Soucek and Zelnick's expression for the pressure change across a discharge port, derived by setting the rate of momentum change equal to the net force, became

$$\frac{P_d - P_u}{w V_u^2/2g} = 2 \frac{q}{Q_u} (1 + k_j) - 2 \left[\frac{q}{Q_u}\right]^2 . \qquad (18)$$

For an intake port they wrote

$$\frac{P_u - P_d}{w V_d^2/2g} = 2 \frac{q}{Q_d} (1 + k_i) - 2 \left[\frac{q}{Q_d}\right]^2 \qquad (19)$$

where k_i has the same meaning as k_j but refers to an intake port.

Soucek and Zelnick pointed out if k_j in Equation 18 or k_i in Equation 19 is taken as unity, which is equivalent to considering the unbalanced port pressure is zero, the value of the pressure change, $P_d - P_u$ or $P_u - P_d$, will equal twice the difference between the velocity heads upstream and downstream from the port.

McNown (27, p. 1), in a discussion of the mechanics of manifold flow based on studies conducted under his supervision, said:

> The complexity of the flow patterns at branch points precludes rigorous analysis, but a general understanding can be obtained from a combination of experimental results with those of simplified analyses.

He also stated even though the branch points may be so close together that mutual interactions of successive junctions affect the pressure changes and losses at the junction, a useful simplification can be made by considering a single branch point in a conduit in which the flow is otherwise uniform throughout a considerable distance upstream and downstream from the junction.

In a manner similar to that of Soucek and Zelnick, McNown stated that in writing the momentum equation for dividing flow at a junction, a term representing either the component of the resultant momentum in the direction of conduit flow or the force required to reduce this component of momentum to zero must be included. McNown considered this force, F, positive in the upstream direction and wrote the following momentum equation for frictionless, right-angled dividing flow

(Fig. 3a):

$$\frac{P_d - P_u}{wV_u^2/2g} = 2\left[1 - \left(\frac{V_d}{V_u}\right)^2 - \frac{F}{\rho Q_u V_u}\right] . \qquad (20)$$

For combining flow (Fig. 3b) he wrote:

$$\frac{P_u - P_d}{w\,V_d^2/2g} = 2\left[1 - \left(\frac{V_u}{V_d}\right)^2 + \frac{F}{\rho Q_d\, V_d}\right] . \qquad (21)$$

In a discussion following Soucek and Zelnick's article, McNown indicated Equations 20 and 21 are equivalent to Equations 18 and 19 if

$k_j = 1 - \frac{F}{\rho q V_u}$ and $k_i = 1 - \frac{F}{\rho q V_d}$.

McNown wrote the following energy equation for dividing flow:

$$\frac{P_d - P_u}{w\,V_u^2/2g} = 1 - \left[\frac{V_d}{V_u}\right]^2 - \frac{\Delta H}{V_u^2/2g} . \qquad (22)$$

For combining flow, he wrote

$$\frac{P_u - P_d}{w\,V_d^2/2g} = 1 - \left[\frac{V_u}{V_d}\right]^2 + \frac{\Delta H}{V_d^2/2g} \qquad (23)$$

where ΔH represents the difference between the total head losses and the losses observed in normal conduit flow.

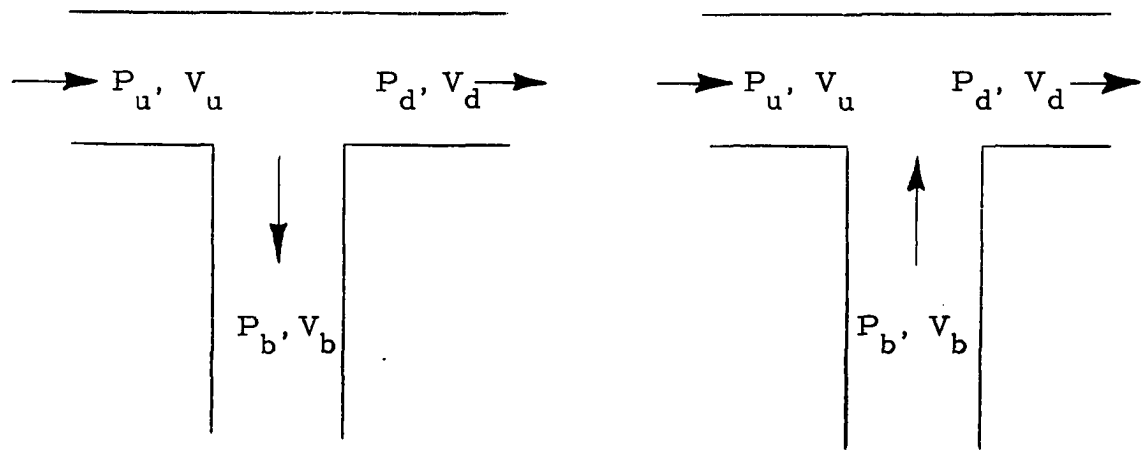

a. Dividing flow b. Combining flow

Fig. 3. Definition sketch for manifold flow

Lack of knowledge of the force, F, and the head loss, ΔH, or the coefficients, k_j and k_i, makes a direct application of Equations 18 through 23 impossible without recourse to experiment.

Experiments under the supervision of McNown were made using a brass pipe with an inside diameter of 2.06 inches for the main conduit. The laterals were made from a similar pipe and brass tubing 1 inch and 1/2 inch in diameter. In all cases the intersection of the lateral with the main duct was sharp-edged. Water was supplied to the various pipes from a constant-level tank.

McNown summarized the results of the experiments by dimensionless curves which are reproduced in Figures 4 and 5. In these

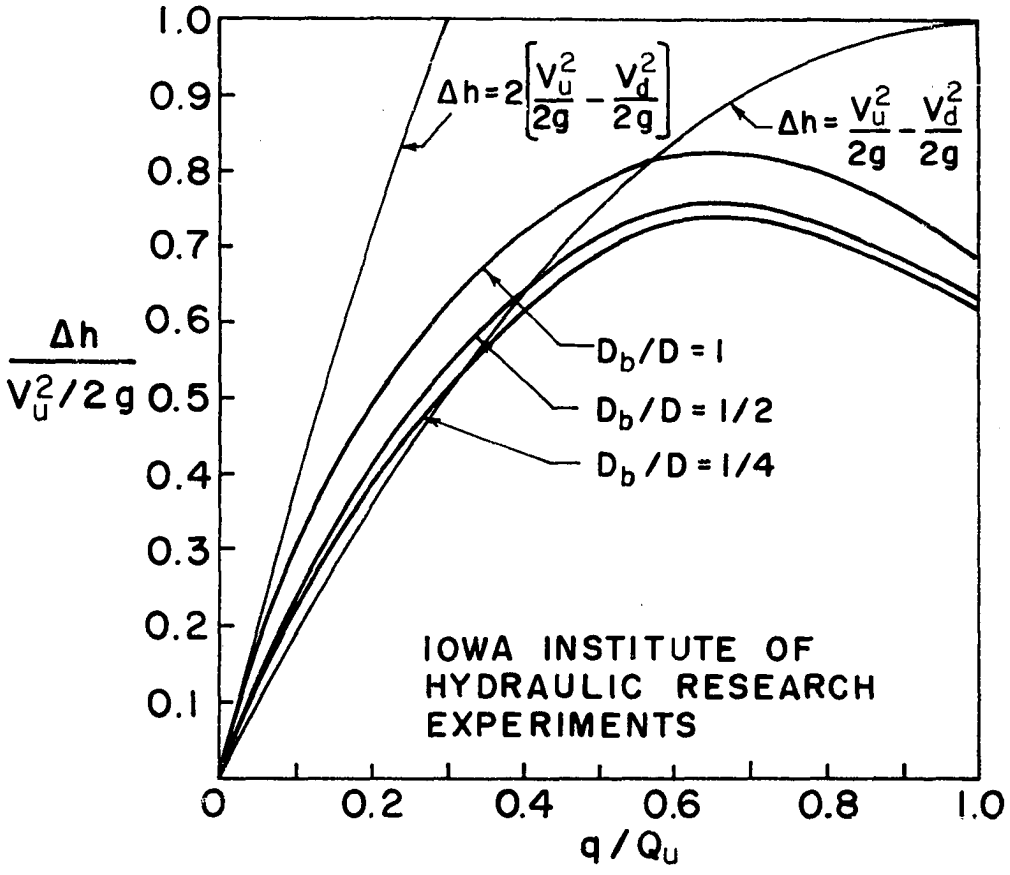

Fig. 4. Change in piezometric head in the conduit for dividing flow

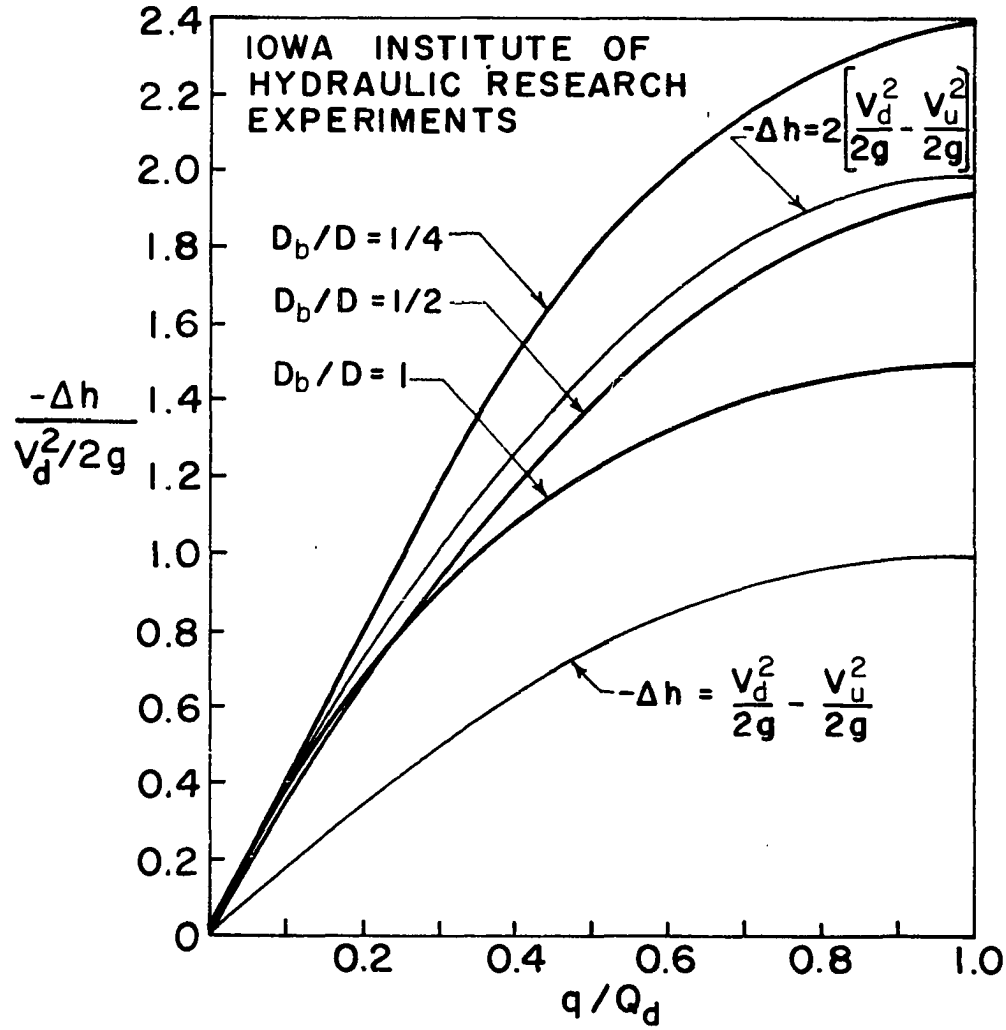

Fig. 5. Change in piezometric head in the conduit for combining flow

figures, curves representing the experimental data are compared with two theoretical curves. These theoretical curves were computed with Equations 20 through 23 by letting $F = \Delta H = 0$. Hence, the lower computed curves in Figures 4 and 5 are curves in which the change in static pressure head is represented by one times the difference in velocity head upstream and downstream of the junction. The upper computed curves in these figures are curves in which the change in static pressure head is represented by two times the change in velocity head upstream and downstream of the junction.

Figures 4 and 5 indicate the ratio of the diameter of the branch lateral to the diameter of the main duct, D_b/D, has little effect on the static pressure change for values of q/Q less than 0.2. It also appears the change in static pressure could be closely represented by a constant times the change in velocity for all values of q/Q less than 0.2.

Horlock (16) made an analysis for the flow from a longitudinal slot in a manifold (Fig. 6) by writing the following momentum equation:

$$-A\left[\frac{\partial P}{\partial x}\right] dx = \frac{\partial}{\partial x}(\rho AV^2)\,dx - u\,\frac{\partial}{\partial x}(\rho AV)\,dx + \tau \pi D\,dx \qquad (24)$$

in which τ = frictional force per unit area of duct wall

$$= \frac{A}{\pi D}\,\frac{dP}{dx} = f\,\frac{Aw}{\pi D^2}\,\frac{V^2}{2g}\,.$$

Equation 24 simplifies to

$$-\frac{1}{w}\frac{dP}{dx} = \frac{(2V - u)}{g}\frac{dV}{dx} + \frac{fV^2}{D\,2g}. \qquad (25)$$

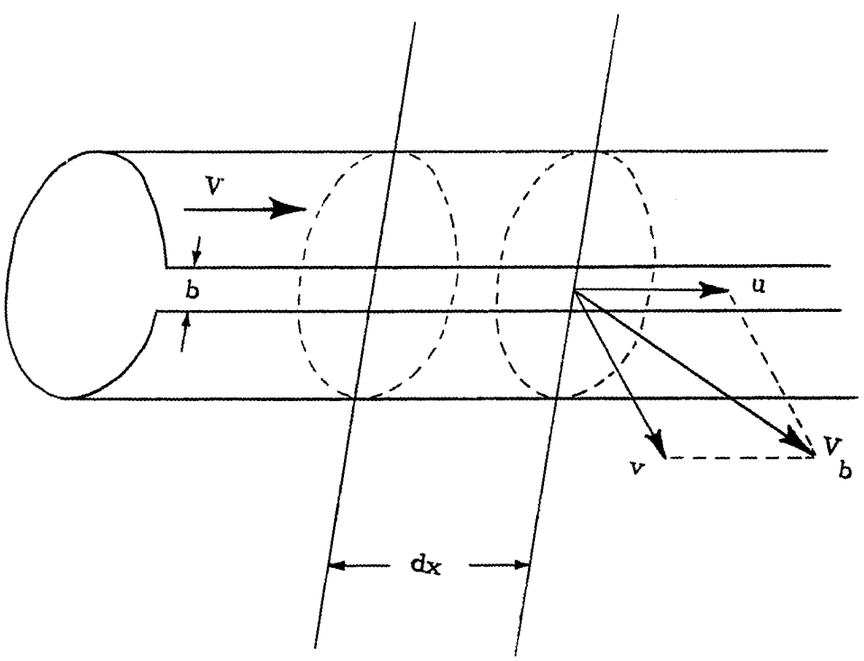

Fig. 6. Discharge from a manifold with longitudinal slot

Horlock assumed the normal velocity of discharge, v, will be determined by

$$P = \frac{1}{2}\rho v^2 \qquad (26)$$

and stated the static pressure, P, can be eliminated from Equation 25 by two different assumptions: (1) the discharged fluid leaves with its longitudinal velocity unchanged, u = V, or (2) the discharge velocity is normal to the manifold, u = 0.

Horlock combined Equations 25 and 26 with the equation of continuity

$$VA = (V + dV)\, A + vb\, dx$$

and derived a second-order differential equation for the longitudinal velocity in the manifold:

$$\frac{A^2}{b^2} \frac{d^2V}{dx^2} \frac{dV}{dx} + (2V-u) \frac{dV}{dx} + \frac{fV^2}{2D} = 0 . \qquad (27)$$

If u = V is substituted in Equation 27, it becomes similar to Equation 11 derived by Keller. Horlock assumed the discharge flow leaves the manifold with unchanged longitudinal velocity, u = V, and obtained a solution to Equation 27 in terms of V/v, the ratio of the longitudinal velocity in the manifold to the normal discharge velocity. Experiments confirming his theoretical analysis were conducted on a 3/4-inch I. D. brass pipe with 3/16-inch diameter holes drilled at 1-inch spacing along the pipe. He did not state what fluid was used in the tests.

Horlock's analysis was based on constant values of the discharge

coefficient and friction factor. He commented the friction factor in a closed-end manifold will increase near the dead end as the velocity approaches zero.

The velocity distribution given by Equation 27 is independent of the static pressure level; hence the manifold velocity distribution is a function of the length of the manifold. Therefore, the discharge or intake distribution, and consequently the static pressure distribution, for a manifold or perforated duct will remain the same for all levels of static pressure.

The intake or discharge distribution is independent of the static pressure or total flow rate level only if the friction factor and coefficient of discharge remain constant. Dow (3) pointed out the intake or discharge variation will be altered if there is a variation in the friction factor. The intake or discharge variation also will be altered if there is a variation in the coefficient of discharge. However, in many practical applications of perforated ducts the friction factor and coefficient of discharge may be considered constant along the length of the duct. From a practical viewpoint, this means a perforated duct designed for uniform discharge or intake per unit length will have a uniform discharge or intake regardless of the static pressure level. Furthermore, a nonuniform distribution of discharge or intake will retain the same nonuniformity at all static pressure levels.

ANALYSIS OF STATIC PRESSURE CHANGE IN A PERFORATED DUCT

The preceding review of literature indicated the static pressure change in a perforated duct can be expressed as the sum of the static pressure change caused by friction and a static pressure change accompanying the increase or decrease of velocity in the duct. If the velocity is increasing in the direction of flow, the change in static pressure accompanying the acceleration of the fluid adds to the friction loss. If the velocity is decreasing in the direction of flow, the change in static pressure accompanying the deceleration of the fluid tends to offset the friction loss. This latter effect is referred to as static pressure regain. No descriptive term has been applied to the former effect.

The effects of friction in fluid flow have been studied in detail, but less attention has been given to the pressure change accompanying the acceleration or deceleration of fluid that occurs as a portion of the fluid enters or leaves through a perforated duct. The following is an analysis of static pressure change associated with velocity change. Figure 7 represents a perforated duct in which fluid entering through a perforation combines with fluid in the duct. The impulse-momentum equation for this frictionless combining flow system can be written as

$$m_d V_d - m_u V_u - m_b V_b \cos \alpha = Ft. \qquad (28)$$

The force, F, in Equation 28 is the resultant horizontal force on the fluid (Fig. 8).

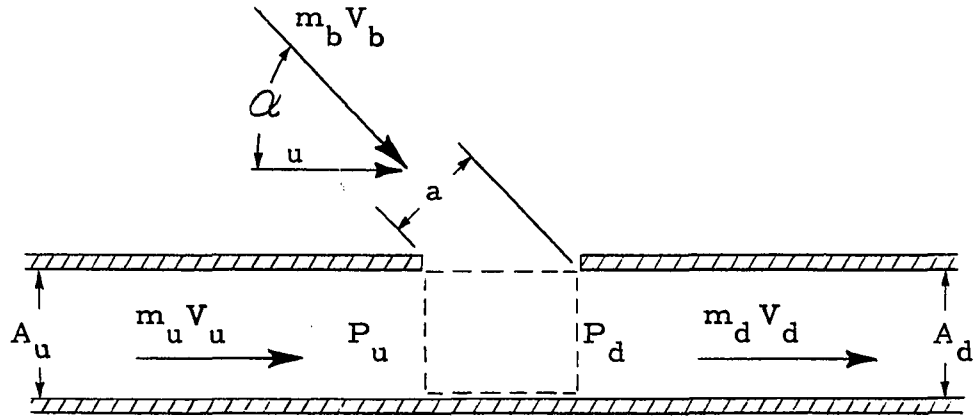

Fig. 7. Diagram for frictionless combining flow in a perforated duct

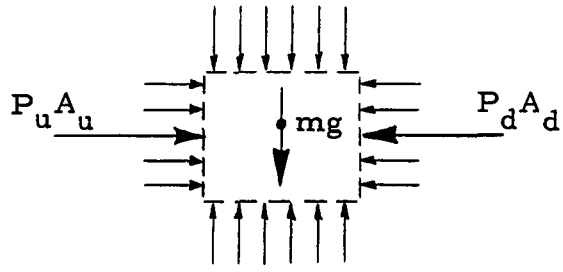

Fig. 8. Forces on element of fluid in a perforated duct

Substitution of $P_u A_u - P_d A_d$ for F and division by t in Equation 28 gives

$$\frac{m_d V_d}{t} - \frac{m_u V_u}{t} - \frac{m_b V_b}{t} \cos \alpha = P_u A_u - P_d A_d . \quad (29)$$

Since $\frac{m}{t}$ = mass per unit time, $\frac{m}{t}$ can be replaced by ρVA; and Equation 29 becomes

$$\rho A_d V_d^2 - \rho A_u V_u^2 - \rho a V_b^2 \cos \alpha = P_u A_u - P_d A_d , \quad (30)$$

which simplifies for a duct of constant cross section to

$$\rho V_d^2 - \rho V_u^2 - \rho \frac{a}{A} V_b^2 \cos \alpha = P_u - P_d \quad (31)$$

where $A = A_u = A_d$.

Substitution of $\frac{w}{g}$ for ρ in Equation 31 gives

$$\frac{w}{g} V_d^2 - \frac{w}{g} V_u^2 - \frac{w}{g} \frac{a}{A} V_b^2 \cos \alpha = P_u - P_d$$

or

$$\frac{V_d^2}{g} - \frac{V_u^2}{g} - \frac{a}{A} \frac{V_b^2}{g} \cos \alpha = \frac{P_u - P_d}{w} = -\Delta h, \quad (32)$$

which can be written in terms of velocity heads as

$$2 \left[\frac{V_d^2}{2g} - \frac{V_u^2}{2g} \right] - \frac{2a}{A} \frac{V_b^2}{2g} \cos \alpha = -\Delta h. \quad (33)$$

Equation 33 is an expression for the static pressure change in a perforated duct accompanying the change in velocity caused by the intake of fluid through the perforated wall.

Since the preceding development was based on frictionless flow, a term representing friction losses must be added to Equation 33 if friction is considered. The usual practice has been to assume the friction loss in a perforated pipe or duct can be considered equal to the normal friction loss observed when there is no flow through the perforated wall. This is a reasonable assumption when the area of the intake or discharge openings is a small percentage of the total duct wall area. Hence, the equation for head loss in a perforated duct for combining flow when friction is considered is

$$-{}_u h_d = 2 \left[\frac{V_d^2}{2g} - \frac{V_u^2}{2g} \right] - \frac{2a}{A} \frac{V_b^2}{2g} \cos \alpha + {}_u(h_f)_d. \quad (34)$$

When Equation 34 is written in differential form, it becomes

$$-\frac{dh}{dx} = 2 \frac{d}{dx} \left[\frac{V^2}{2g} \right] - \frac{2a}{A} \frac{V_b^2}{2g} \cos \alpha + \frac{dh_f}{dx} . \quad (35)$$

Since $aV_b = q$, $\frac{q}{A} = \frac{dV}{dx}$, and $V_b \cos \alpha = u$,

Equation 35 reduces to

$$-\frac{dh}{dx} = \frac{2V}{g}\frac{dV}{dx} - \frac{u}{g}\frac{dV}{dx} + \frac{dh_f}{dx} \tag{36}$$

or

$$-\frac{dh}{dx} = \left[\frac{2V - u}{g}\right]\frac{dV}{dx} + \frac{dh_f}{dx} \quad . \tag{37}$$

An identical analysis can be made for dividing flow; however, in dividing flow the static pressure regain accompanying the decrease in velocity tends to offset the friction loss. Hence, for dividing flow Equation 37 becomes

$$\frac{dh}{dx} = -\left[\frac{2V - u}{g}\right]\frac{dV}{dx} + \frac{dh_f}{dx} \quad . \tag{38}$$

Two special cases of Equations 37 and 38 are of interest, that is, $u = 0$ and $u = V$. If $u = V$, the change in static pressure associated with the change in velocity is equal to the rate of change of velocity head. On the other hand, if $u = 0$, which is equivalent to $\alpha = 90$ degrees (fluid entering or leaving normal to the direction of flow), the static pressure change associated with the change in velocity is equal to twice the rate of change of velocity head.

If, in the general case, u is a constant proportion of V, Equations 37 and 38 can be written

$$\frac{dh}{dx} = -\frac{KV}{g}\frac{dV}{dx} \pm \frac{dh_f}{dx} \tag{39}$$

where KV = 2V-u.

The minus sign on the friction term in Equation 39 applies to combining flow in which the static pressure change associated with velocity change adds to the static pressure change associated with friction. The plus sign on the friction term applies to dividing flow in which the static pressure change associated with velocity change tends to offset the static pressure change associated with friction.

For a given increment of duct length Equation 39 can be written

$$\Delta h = - K \left[\frac{V_d^2}{2g} - \frac{V_u^2}{2g} \right] \pm \Delta h_f$$

or

$$\Delta h = -K \frac{V_d^2}{2g} \left[1 - \frac{V_u^2}{V_d^2} \right] \pm \Delta h_f \quad . \tag{40}$$

Since $$\frac{V_u}{V_d} = \frac{Q_u}{Q_d} = \frac{Q_d - q}{Q_d} = 1 - \frac{q}{Q_d} \quad ,$$

Equation 40 can be written in terms of the flow ratio, q/Q_d, as

$$\Delta h = -K \frac{V_d^2}{2g} \left[\frac{q}{Q_d} \left(2 - \frac{q}{Q_d} \right) \right] \pm \Delta h_f \quad . \tag{41}$$

Equation 41, arranged in dimensionless form as

$$\frac{\Delta h \pm \Delta h_f}{V_d^2 / 2g} = - K \left[\frac{q}{Q_d} \left(2 - \frac{q}{Q_d}\right) \right], \qquad (42)$$

will be used later as the basis for plotting the experimental data.

EQUIPMENT AND EXPERIMENTAL PROCEDURE

A perforated metal duct of the following specifications was selected for this study:

Diameter of duct	5 inches
Diameter of perforations	0.078 inch
Center to center distance of perforations and arrangement	0.125 inch staggered
Percent open area	36%
	76 holes per sq. inch
Type of metal	No. 22 gage cold rolled black iron
Length of each section	3 feet

The perforations were sharp-edged on the inside surface of the duct wall and slightly rounded on the outside. Butt joints, secured with metal draw bands, were used in assembling the 3-foot sections of duct into longer lengths. The test duct was connected to a 4-foot-square plenum chamber, which served as the transition section between the duct and fan. The inlet or outlet of the fan could be connected to the plenum chamber to operate the duct under either suction or pressure.

Air flow quantities were determined by observing the static pressure drop across perforated metal sheets as outlined by

Shedd (32). The perforated metal sheets used in this study were calibrated in place by making a pitot tube traverse in the 5-inch diameter test duct (Appendix A).

To determine the air intake or discharge at a point on the duct, collector units (Fig. 9), consisting of plywood boxes with dimensions of 6 x 14 x 14 inches, were placed over each opening and sealed to the duct with masking tape. These collector units contained perforated metal sheets for determining air flow as outlined in Appendix A. A large sheet of perforated metal in a transition section attached to the end of the duct was used to determine the air flow rate in the duct. The air flow rate in the duct was varied by adjusting sliding-gate valves installed at least 20 diameters upstream and 20 diameters downstream from the test section.

Static pressure taps were placed 18 inches upstream and 18 inches downstream from a given air opening on the duct. Small tubing from each pressure tap (Fig. 9) was connected to a panel in order that all readings could be made without moving the manometer. A traverse of the duct with a standard pitot tube indicated the static pressure was constant along a diameter anywhere beyond 14 inches downstream from an opening into the duct. On the upstream side a constant static pressure along a diameter was found to exist up to a point adjacent to the opening. The static pressures observed at these

Fig. 9. Collector unit containing perforated metal sheet used to measure the air intake or discharge at an opening in a 5-inch diameter perforated metal duct

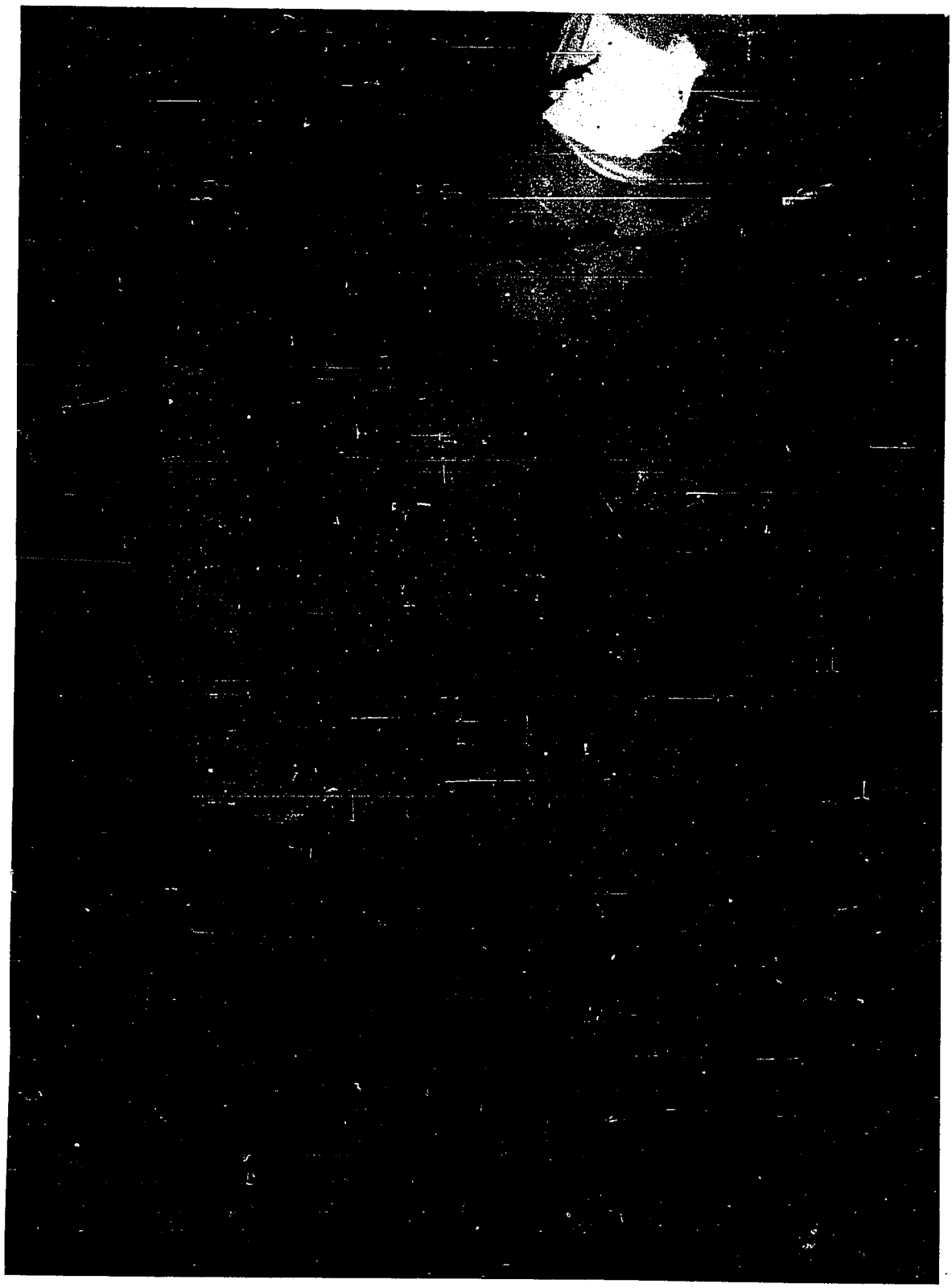

points in the duct with the pitot tube aligned with the static pressures observed from readings obtained using the static pressure taps placed on the outside wall surface of the duct.

Pressures and pressure differentials of less than 2 inches of water were read with a Meriam inclined manometer graduated in 0.01 inches of water. Pressures and pressure differentials above 2 but less than 4 inches of water were read with a Dwyer diaphragm type of gage graduated in 0.1 inches of water. Pressures above 4 inches of water were read with a vertical water manometer graduated in 0.1 inches.

Although the objective of this study was to establish a relationship between the static pressure gradient and air flow in a perforated duct in order to analyze pressures and air flows in ventilation ducts in grain piles, the experimental duct was not buried in grain. It appeared the effect of grain on a duct could be accounted for separately, not discounting, however, the possibility that additional experiments might be necessary. Essentially this study was concerned with the inside of the duct and only indirectly concerned with the outside surface of the duct wall. Since grain ventilation ducts can be operated either under suction or pressure, both systems were studied.

A group of suction tests on single openings was conducted in an attempt to establish a relationship between the rate of change of static pressure in the duct and the rate of change of air flow in the duct.

In these combining flow tests the quantity of air entering the duct at a given opening was varied by adjusting the amount of open area on the duct. The maximum amount of opening into the duct used at any point was 12 circumferential rows of perforations, approximately 1.25 inches of duct length. Twelve circumferential rows of perforations equaled an open area of 7.05 square inches.

The air flow rate in the duct was varied by adjusting the sliding-gate valves and/or adjusting a valve in the transition section between the duct and fan. The air flow rates were varied to obtain a range of values of the flow ratio, q/Q_d. The flow rate downstream from an opening, Q_d, was used in this ratio to avoid the ratio, $q/0$, at the dead end.

During a single test the following data were recorded:

1. Static pressure drop across the perforated sheet in the transition section at the end of the duct for determination of the upstream air flow rate.
2. Static pressure drop across the perforated sheet in the collector units for determination of the quantity of air entering the duct openings.
3. Static pressure differential along 3 feet of duct (18 inches upstream and 18 inches downstream of each opening).

The observed static pressure differentials along 3 feet of duct were corrected for friction according to the friction chart in Appendix B

and then compared with the value of the change in velocity head accompanying the increase of flow in the duct. From this comparison a prediction equation for the rate of change of static pressure was established for combining flow.

After establishment of the prediction equation for combining flow from the study of single openings, the prediction equation was used to compute the static pressure in a length of duct with a series of 20 uniform openings spaced on 6-inch centers. This computation required an auxiliary air flow calibration of the perforations in the test duct wall (Appendix C). The static pressures in a length of the duct containing 20 uniform openings then were observed for comparison with the computed values.

The prediction equation also was used to compute the static pressures associated with a uniform air intake at 20 openings along the length of the duct. These computed static pressures were established in the duct by adjustment of the openings with the aid of the auxiliary air flow calibration of the perforations in the test duct wall. The auxiliary air flow calibration was used to determine the quantity of air entering each opening after final adjustment of the openings. These determined air quantities were compared with the uniform air intake used in the computations.

With one exception tests similar to those described above were

conducted with the duct under pressure. The exception was the elimination of the series of tests on single openings.

RESULTS - SUCTION SYSTEM

The static pressure differentials observed along 3 feet of duct for the series of suction tests on single openings were corrected for duct friction according to the friction chart in Appendix B. These corrected static pressure differentials were compared with the change in velocity head in the duct in a dimensionless plot based on Equation 42. This dimensionless plot is shown in Figure 10. Two arbitrary values of the constant, K, in Equation 42 were plotted in Figure 10 for comparison with the experimental data. In the upper curve where K = 2, the change in static pressure associated with the change in velocity is represented by two times the change in velocity head. In the lower curve where K = 1, the change in static pressure associated with the change in velocity is represented by one times the change in velocity head. These factors usually are applied to the change in velocity head in equations appearing in the literature reviewed.

Experimental data were obtained for values of the flow ratio, q/Q_d, between 0.005 and 1.0; and points representing the data were plotted in Figure 10. Since most of the experimental data were between a flow ratio of 0.01 to 0.1, this region was used in fitting a curve to the experimental points. The points plotted as open circles were disregarded since they represent observed static pressure

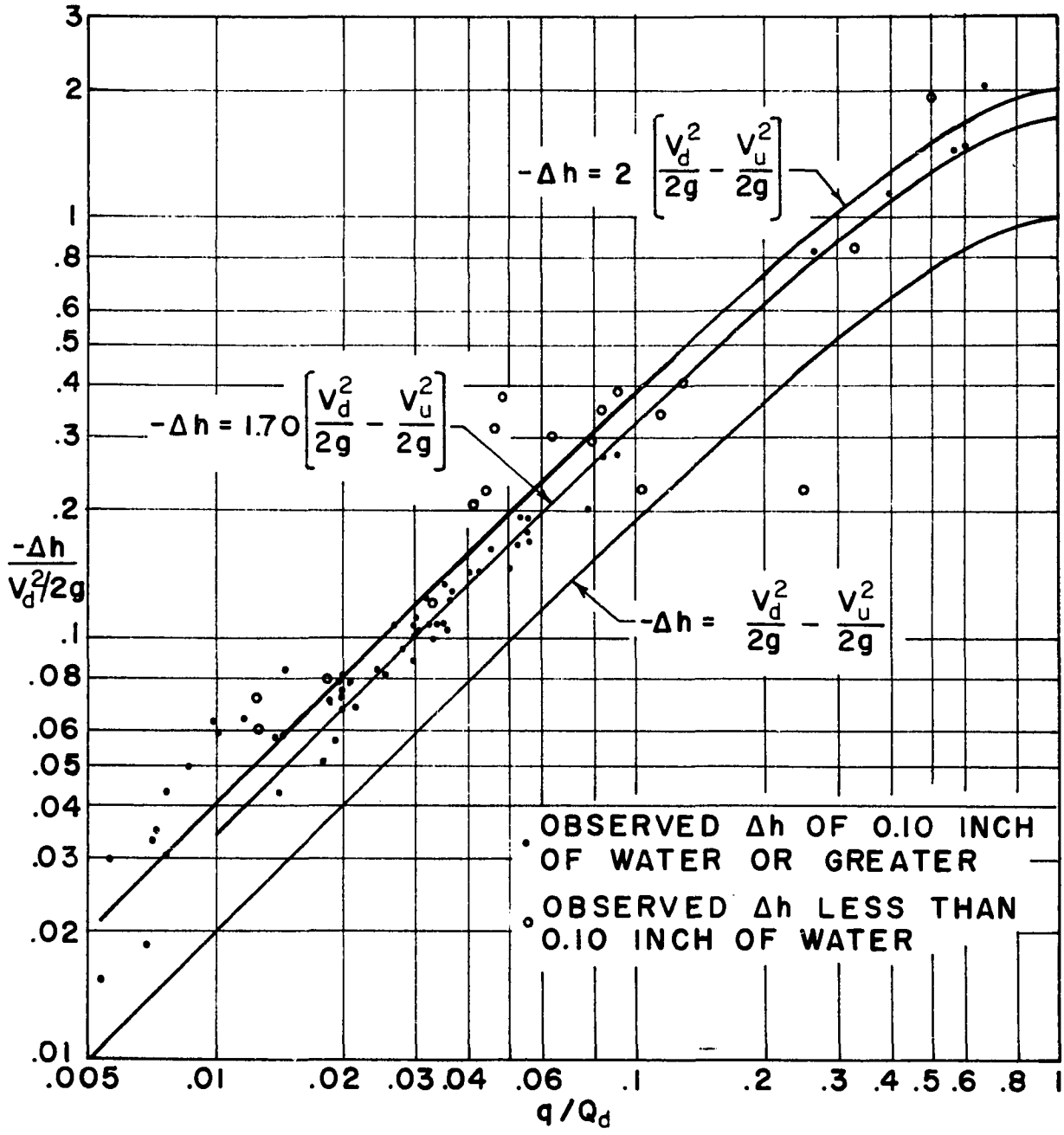

Fig. 10. Change in static pressure head in a 5-inch perforated metal duct for combining flow

differentials of less than 0.1 inches of water, which resulted in considerable experimental error as indicated by the scatter of these points. The scatter of the points below a flow ratio of 0.01 also indicated considerable experimental error. Below a flow ratio of 0.01 the static pressure change caused by friction nearly equaled the observed static pressure differential. The small value of the observed static pressure differential which remained after the correction for friction was applied could not be relied on to represent the static pressure change associated with the change in velocity. Near equality between the friction loss and observed pressure loss also explained the increased scatter of the points as the flow ratio approached 0.01.

A curve was drawn through the average point of the experimental points between a flow ratio of 0.01 and 0.1 and parallel to the curves representing one and two times the change in velocity head. This experimentally-determined curve lay 0.7 of the distance between the curves representing one and two times the change in velocity head. In this curve the static pressure change was represented by 1.70 times the change in velocity head. The equation for the static pressure change in the test duct for combining flow became

$$-{}_{u}h_{d} = 1.70 \left[\frac{V_d^2}{2g} - \frac{V_u^2}{2g} \right] + \text{friction loss.}$$

On the basis of this result the following equation for the rate of static pressure change in a duct with an air intake along its length was written:

$$-\begin{matrix}\text{Rate of static}\\ \text{head change}\end{matrix} = K_s\left[\begin{matrix}\text{Rate of velocity}\\ \text{head change}\end{matrix}\right] + \begin{matrix}\text{Rate of friction}\\ \text{head loss.}\end{matrix} \qquad (43)$$

Although this type of equation was indicated in the literature reviewed, the constant, K_s, by which the acceleration term is multiplied could not be predicted. Some investigators multiplied the acceleration term by one; others multiplied the acceleration term by two. An additional experimentally-determined head loss term often was introduced to compensate for any discrepancies between analytical considerations and experimental observations.

If the friction loss is represented by the Darcy-Weisbach formula, Equation 43 can be written as

$$-\frac{dh}{dx} = K_s \frac{d}{dx}\left[\frac{V^2}{2g}\right] + \frac{fV^2}{D\,2g}$$

or

$$-\frac{dh}{dx} = K_s \frac{V}{g}\frac{dV}{dx} + \frac{fV^2}{D\,2g}\,. \qquad (44)$$

The substitution of Q/A for V in Equation 44 gives

$$-\frac{dh}{dx} = K_s \frac{Q}{A^2 g} \frac{dQ}{dx} + \frac{fQ^2}{A^2 D 2g} \tag{45}$$

which can be simplified to

$$\frac{dh}{dx} = -M_s q Q - N Q^2 \tag{46}$$

where

$$M_s = \frac{K_s}{A^2 g}$$

$$N = \frac{f}{A^2 D 2g} .$$

A solution of Equation 46 for an unknown air intake along a duct can be made in terms of a velocity or flow ratio as indicated by Horlock (16, p. 750). Since this type of solution does not lead directly to the prediction of the static pressure gradient or flow rate along the duct, it is more convenient to perform a numerical point-by-point evaluation of Equation 46.

The solution of Equation 46 for an unknown air intake along a perforated duct requires an auxiliary calibration to relate static pressure in the duct to air intake through the duct perforations. When this auxiliary calibration is available and the static pressure, h_o, at the zero end opening is known, the quantity, q, entering this opening can be determined from the auxiliary calibration. Since $Q_d = q$ at this

first opening, Equation 46 can be used to compute the change in static pressure from the first to the second opening. The static pressure at the second opening will be the sum of the computed change in static pressure and h_o. The quantity of air entering the second opening can be determined from the auxiliary calibration. The change in static pressure from the second to the third opening then can be computed by the substitution of the new values of q and Q_d in Equation 46. When this procedure is repeated progressively, the static pressure gradient and air intake along the entire length of the duct can be computed.

Since Equation 46 was established from a study of individual openings, it was necessary to check its validity by using it to predict the static pressure gradient for a length of duct containing a series of uniform openings. The static pressure gradient was computed for a length of the test duct containing 20 uniform openings of two circumferential rows spaced 6 inches center to center on the duct by using the preceding procedure and Equation 46 with $K_s = 1.70$. For this computation an auxiliary calibration of the perforations in the test duct wall was necessary and is shown in Figure 17 (Appendix C). A comparison of the computed and observed static pressures for the 20 uniform openings is shown in Figure 11. The air intake as determined by the calibration chart in Appendix C also is indicated in Figure 11.

If the air intake at each opening is to be equal, Equation 46

becomes

$$\frac{dh}{dx} = - M_s q^2 x - N q^2 x^2 \qquad (47)$$

since Q = qx for equal air intake per opening or per unit length. Equation 47 readily integrates to

$$h = - \frac{M_s}{2} q^2 x^2 - \frac{N}{3} q^2 x^3 + h_o. \qquad (48)$$

The selection of a given value of air intake, q, and dead end static pressure, h_o, permits the static pressure at every point along a duct to be computed from Equation 48. If these computed static pressures are established in the duct, the air flow variation in the duct will be linear, i.e., the air intake along the length of the duct will be uniform.

The static pressure gradient for equal air intake at 20 openings on 6-inch centers for the test duct was computed by Equation 48 with $K_s = 1.70$. The area of the openings was adjusted to establish experimentally the computed static pressure gradient in the duct. The adjustment of the openings was facilitated by use of the air intake calibration chart (Fig. 17, Appendix C). After the openings were adjusted, this chart was used to determine the air intake at each opening. In Figure 12 the determined air quantity entering each opening is compared with the uniform air intake used in the computations of the static pressure gradient.

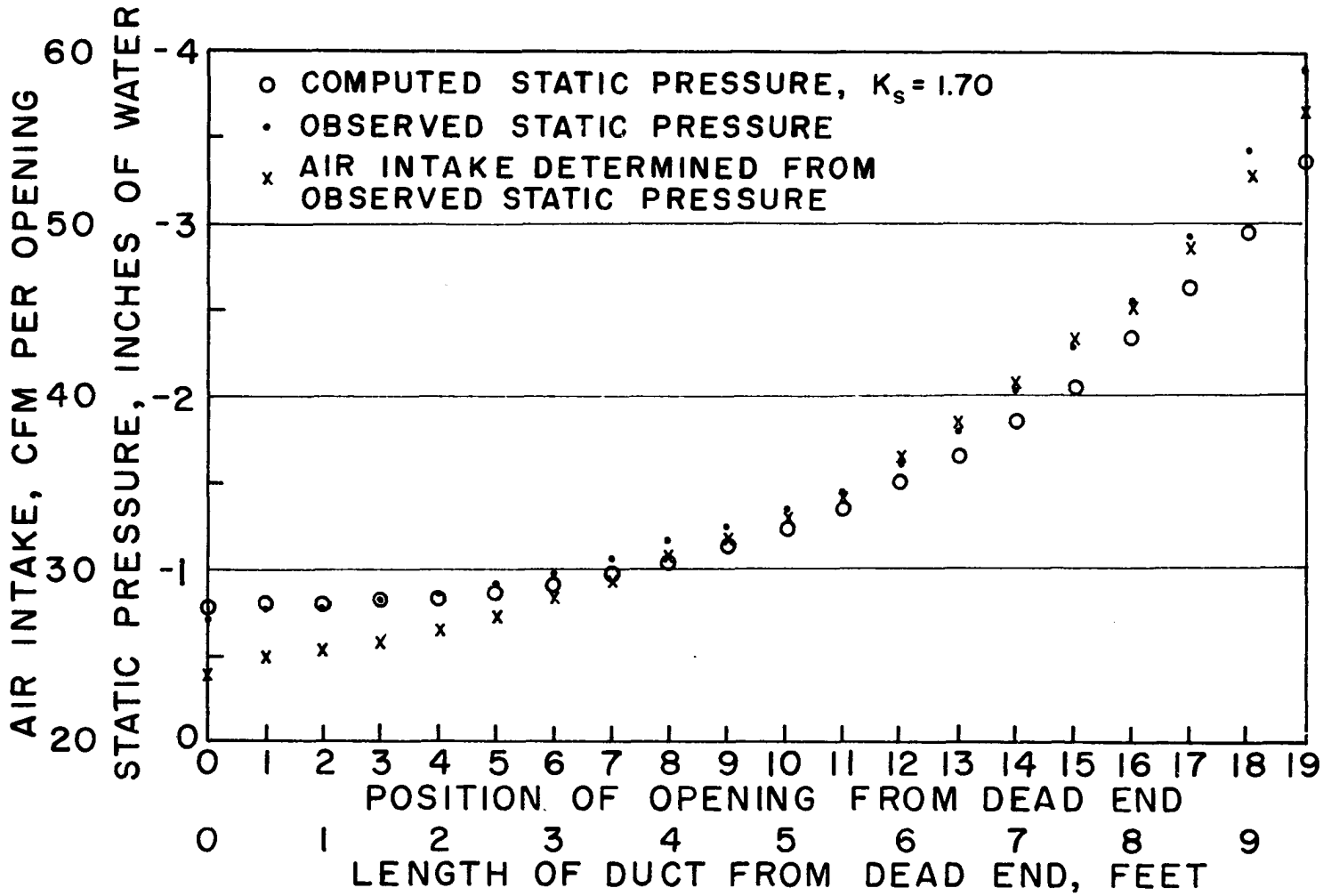

Fig. 11. Static pressure and air intake for 5-inch diameter perforated metal duct with 20 uniform openings of two circumferential rows containing 123 perforations of 0.078-inch diameter

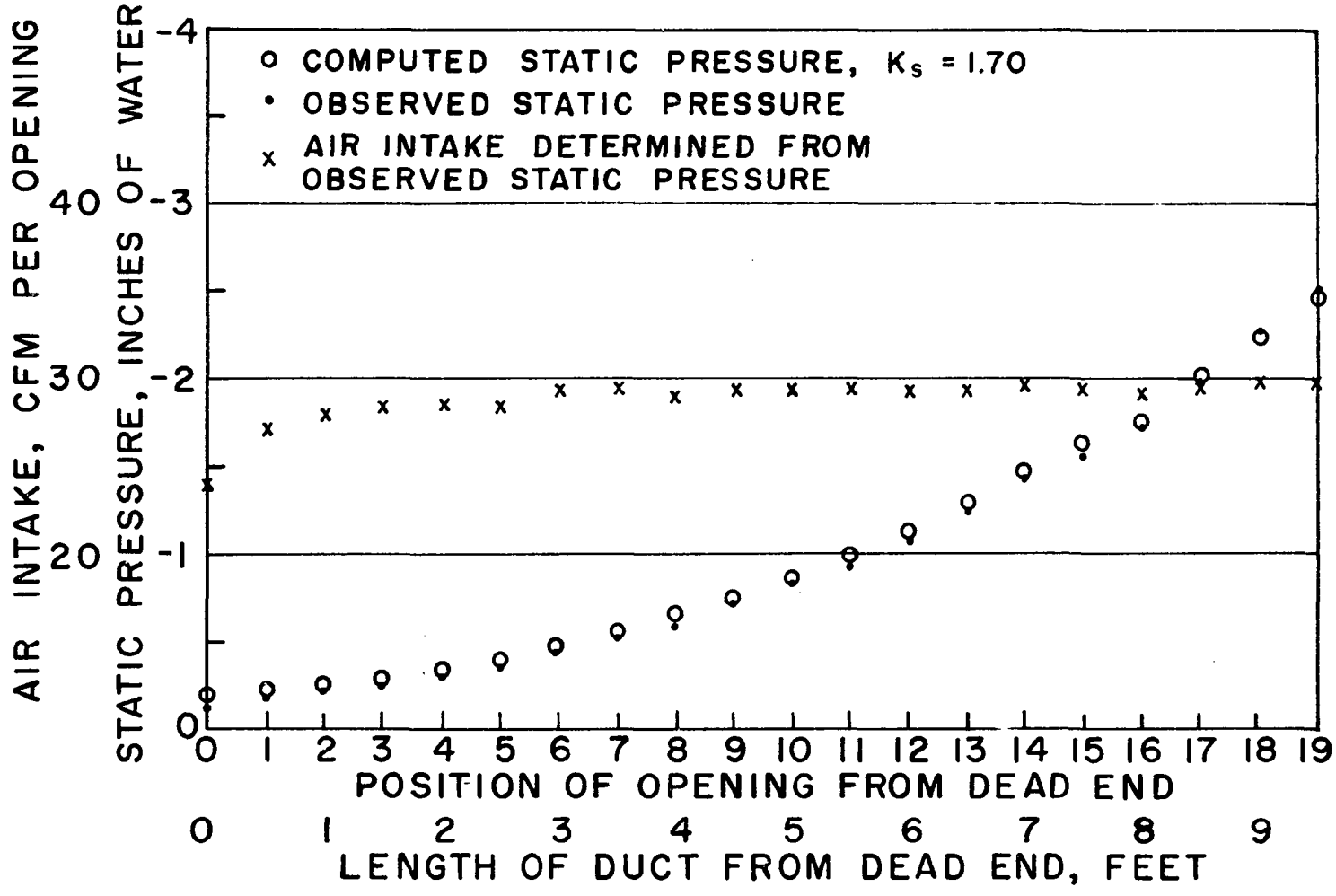

Fig. 12. Static pressure and air intake for 5-inch diameter perforated metal duct with 20 openings proportioned for an air intake of 30 cfm at each opening

RESULTS - PRESSURE SYSTEM

The results of the preceding tests indicated an equation, similar to Equation 43, could be written for the static pressure change in the duct when the duct was under a positive static pressure. This equation is:

$$\begin{matrix}\text{Rate of static} \\ \text{head change}\end{matrix} = -K_p \left[\begin{matrix}\text{Rate of velocity} \\ \text{head change}\end{matrix}\right] + \begin{matrix}\text{Rate of friction} \\ \text{head loss.}\end{matrix} \qquad (49)$$

In Equation 49 the upstream direction is considered the positive direction in order to maintain the positive direction as the direction from the dead end to the fan end.

To determine the constant factor, K_p, to be applied to the change in velocity head for dividing flow, the static pressures were observed for a length of duct with 20 uniform openings. The openings were spaced on 6-inch centers, and each opening consisted of two circumferential rows of perforations. The observed static pressures were compared with values computed using a point-by-point solution of the following equation and the auxiliary calibration for air discharge (Fig. 18, Appendix C):

$$\frac{dh}{dx} = - M_p \, qQ + NQ^2 \qquad (50)$$

where

$$M_p = \frac{K_p}{A^2 g} \quad .$$

In Equation 50 the value of K_p in the constant, M_p, was established by the trial-and-error method. For the first approximation K_p was assumed to be equal to 1.70, as determined from the suction tests. The calculated static pressures using $K_p = 1.70$ were less than the observed values. However, agreement was found for a value of $K_p = 1.50$. This agreement is shown in Figure 13.

The equation for the static pressure under conditions of uniform discharge became

$$h = -\frac{M_p}{2} q^2 x^2 + \frac{N}{3} q^2 x^3 + h_o. \qquad (51)$$

The static pressure gradient for equal air discharge at 20 openings on 6-inch centers for the test duct was computed by Equation 51 with $K_p = 1.50$. The area of the openings was adjusted to establish experimentally the computed static pressure gradient in the duct. The adjustment of the openings was facilitated by use of the air discharge calibration chart (Fig. 18, Appendix C). After the openings were adjusted, this chart was used to determine the air discharge at each opening. In Figure 14 the determined air quantity discharged at each opening is compared with the uniform air discharge used in the computations of the static pressures.

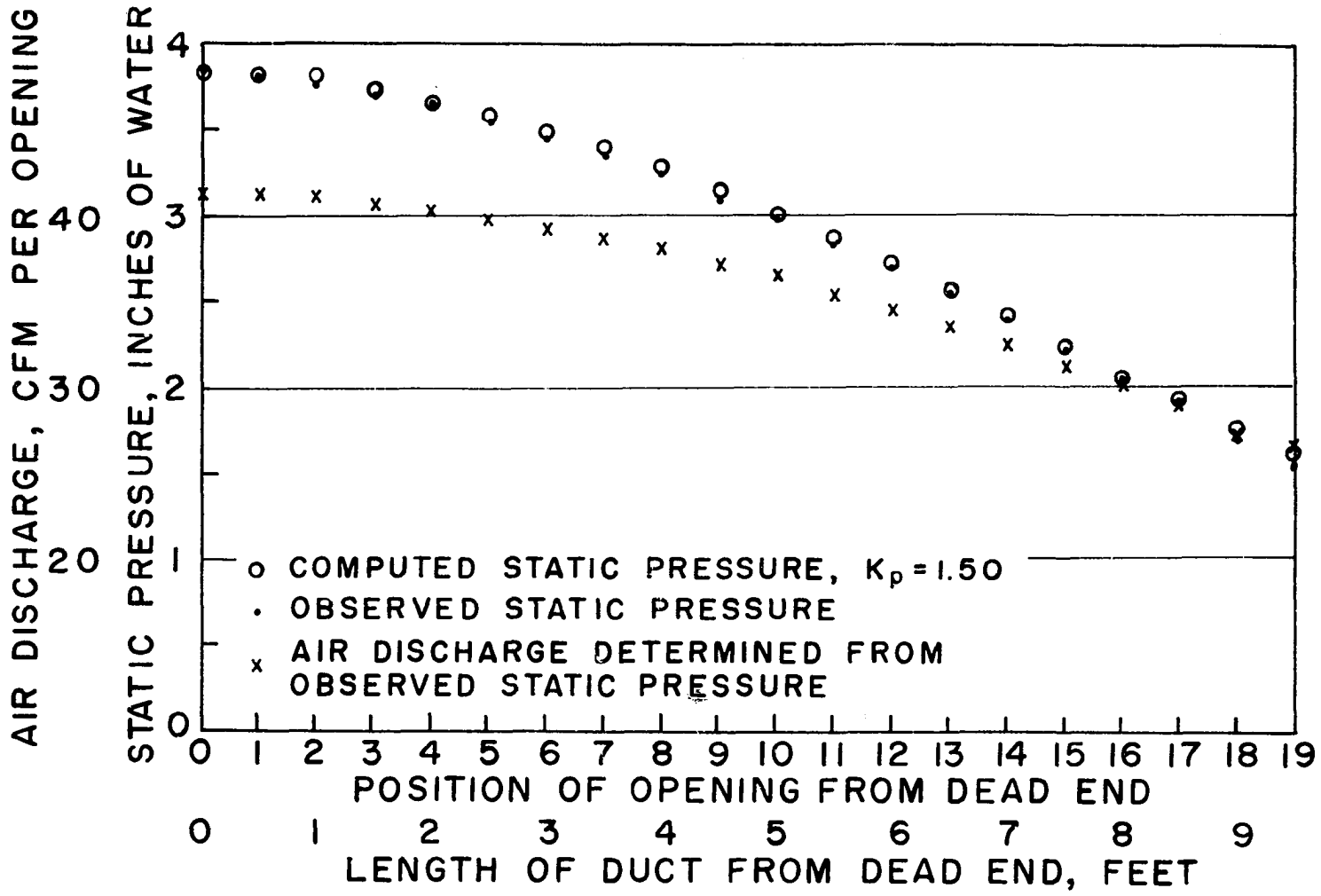

Fig. 13. Static pressure and air discharge for 5-inch diameter perforated metal duct with 20 uniform openings of two circumferential rows containing 123 perforations of 0.078-inch diameter

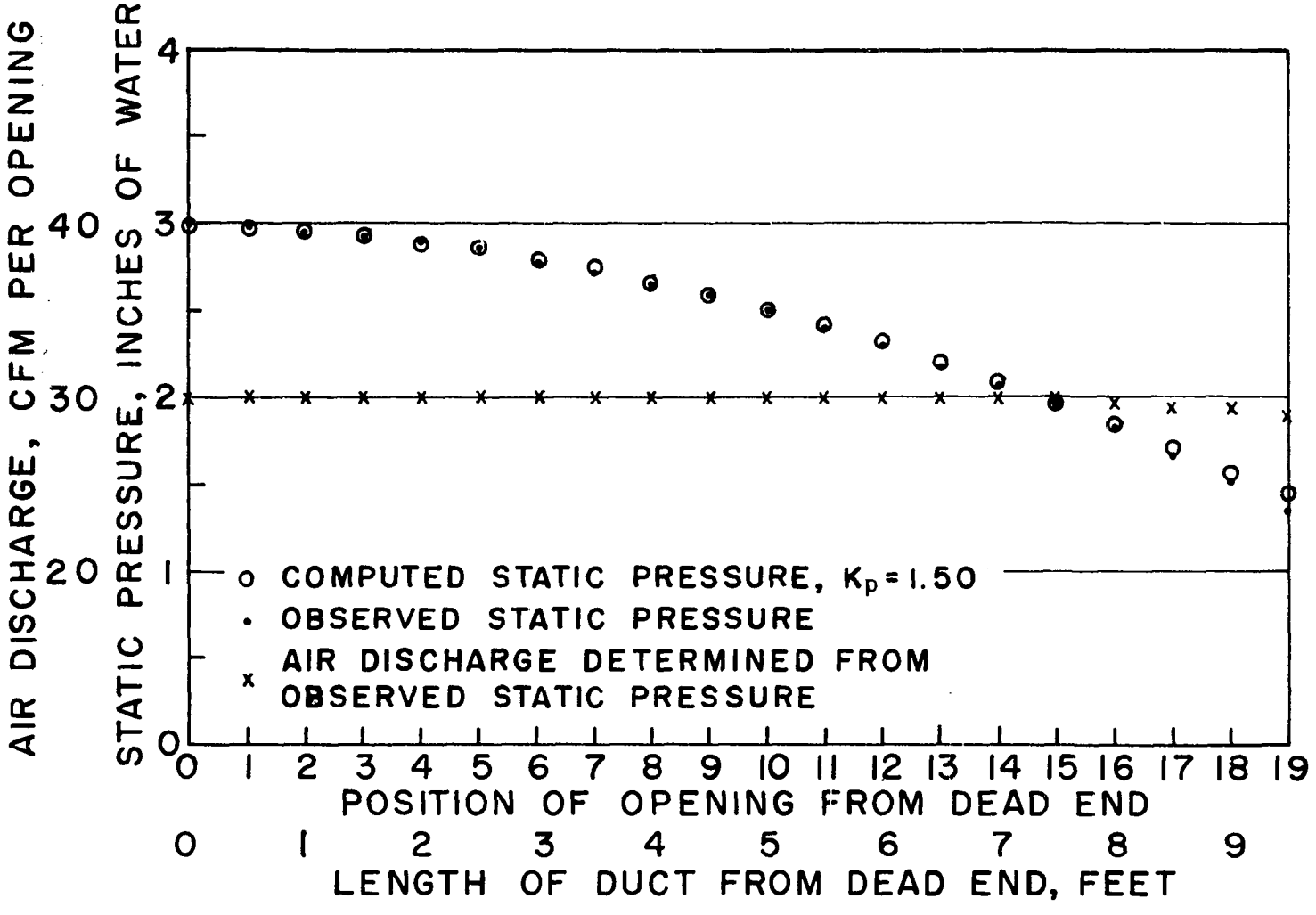

Fig. 14. Static pressure and air discharge for 5-inch diameter perforated metal duct with 20 openings proportioned for an air discharge of 30 cfm at each opening

DISCUSSION

In the development of the equation for static pressure change in a perforated duct the angle, α, the entering fluid makes with the main duct was included as one of the variables. Equation 35,

$$-\frac{dh}{dx} = 2 \frac{d}{dx}\left[\frac{V^2}{2g}\right] - \frac{2a}{A} \frac{V_b^2}{2g} \cos \alpha + \frac{dh_f}{dx},$$

was subsequently derived and is an equation for the rate of static pressure change for combining flow. A branch duct directs fluid into the main duct at an angle nearly equal to the angle the branch makes with the main duct. Favre (7) showed the static pressure change for combining flow could be predicted by the use of the branch angle in the equation for the rate of static pressure change.

Apparently the perforations in a pipe or duct do not direct the fluid into the duct at the 90-degree angle the perforations usually make with the duct wall. Hence the angle, α, for a perforated duct is not defined easily. An attempt was made to observe the angle of air intake through the perforations in the duct used in this study. Smoke was introduced into the air stream, but no definite flow lines could be observed as turbulence near the perforations seemed to disperse the smoke in all directions. A silk thread held in the air stream passing through one perforation indicated the angle, α, decreased as q/Q

decreased; but no accurate measurement of the angle could be made.

The equation for predicting the static pressure change in a perforated duct is composed of two terms: (1) an acceleration or deceleration term and (2) a friction term. The friction loss applied to a perforated duct has been assumed to be equal to the friction loss observed when there is no flow through the perforations. This is a reasonable assumption when the perforations are a small percentage of the total duct wall area. Henderson (13) has presented information on the resistance of perforated metal sheets to air flow when these sheets support grain. His studies showed if a perforated metal sheet supporting grain is to offer any appreciable resistance to air flow in addition to that offered by the grain, the percentage open area of the perforated sheet must be less than about 20 percent. Consequently, a perforated duct designed to control air distribution for grain ventilation by variation of the air openings will have an air opening area of less than 20 percent of the effective duct wall surface area. Therefore, the friction observed with no flow through the perforations can be applied to a perforated duct used to control air distribution in grain ventilation since the area of the perforations will be a small percentage of the total duct wall area.

APPLICATION OF RESULTS

The application of the equation for combining flow

$$\frac{dh}{dx} = - M_s qQ - NQ^2 \tag{46}$$

and the equation for dividing flow

$$\frac{dh}{dx} = -M_p qQ + NQ^2 \tag{50}$$

for computing the air flow distribution along a grain ventilating duct can be made after the values of K_s, K_p, and f included in the constants, M_s, M_p, and N, are assumed or experimentally determined. A solution for an unknown air intake or discharge along the duct is performed by a numerical point-by-point procedure. The auxiliary calibration to relate the static pressure in the duct to the air intake or discharge required in the computations is available; for Henderson (13) has presented information on the air flow resistance of perforated metal sheets supporting grain, Hukill and Ives (20) have analyzed radial air flow resistance of grain, and Shedd (33) has obtained information on the resistance of grain to air flow.

The static pressure associated with a uniform air intake or discharge can be computed since Equations 46 and 50 can be integrated after substituting $qx = Q$. The investigations of Henderson (13), the analysis made by Hukill and Ives (20), and the information of

Shedd (33) then are used to determine the required variation of the air openings along the length of the duct to provide the proper restriction to air flow through the duct wall in order to limit the air intake or discharge to a uniform value.

The following two examples illustrate the application of Equations 46 and 50.

Example 1

Compute the air flow distribution in a cylindrical bin of shelled corn. The air is passed outward from a vertical duct in the center of the bin, and the bin wall is perforated sufficiently to give negligible pressure drop. The following information is given:

Diameter of bin, 16 ft

Depth of shelled corn, 10 ft

Diameter of ventilating duct, 1 ft

Length of ventilating duct, 10 ft

Percent open area of ventilating duct wall, 50%

Static pressure at dead end of duct, 2.500 inches of water

Fan on pressure.

Since a 50 percent open area duct wall will not offer any appreciable resistance to air flow, it will be assumed the static pressure in the duct is dissipated in the $7\frac{1}{2}$-foot radial depth of shelled corn.

A static pressure difference of 2.500 inches of water between 0.5-foot and 8.0-foot radii will force 410 cfm of air per foot of length of duct through the shelled corn. This air flow rate was read from Figure 2 in Hukill and Ives' (20) article. Similarly, the air discharge at every point along the length of the duct can be determined by predicting the static pressure along the length of the duct from Equation 50. If it is assumed that $K_p = 1.50$ and $f = 0.05$, the constants, M_p and N, in Equation 50 for this example become

$$M_p = \frac{2K_p}{A^2 2g} = \frac{(2)\ (1.50)}{(0.785)^2\ (4005)^{2*}} = (0.304)10^{-6}$$

$$N = \frac{f}{A^2\ D2g} = \frac{0.05}{(0.785)^2\ (1)\ (4005)^2} = (0.00507)10^{-6}$$

and Equation 50 can be written as

$$\frac{dh}{dx} = -(0.304)10^{-6}\ q\Omega + (0.00507)10^{-6}\ \Omega^2 \qquad (50a)$$

in which

$\frac{dh}{dx}$ = static pressure change per ft of duct in the direction opposing flow, inches of water

q = volume of air discharged per foot of duct, cfm

*Includes the term, 2g, and the necessary conversion factors to compute h in inches of water when q and Q are in cfm.

Q = accumulative volume of air in duct, cfm.

The static pressure change in the first foot of duct from the dead end is obtained by the substitution of $q = Q = 410$ cfm in Equation 50a. This computed static pressure change algebraically added to the dead end static pressure gives the static pressure to be used at the second foot of length for determining the air discharge at this position. Point-by-point the air flow and static pressure change can be computed for the entire length of the duct. The computations for this example are summarized in Table 2. The air flow distribution along the length of the duct is given in the third column. The air flow varied from 410 cfm per foot at the dead end to only 230 cfm per foot at the fan end. To simplify this example, radial flow was assumed and no attempt was made to account for any diversion from radial flow.

Example 2

Compute the static pressure and determine the required percent of open area for uniform air distribution in a half cylindrical grain ventilation duct installed on the floor center line of a half cylindrical shelled corn storage building. The following information is given:

Length of building, 100 ft

Radius of building, 12 ft

Table 2. Summary of computations for Example 1

x ft	h in-H_2O	q cfm/ft	Q cfm	qQ	Q^2	$-(0.304)10^{-6}qQ$	$(0.00507)10^{-6}Q^2$	dh/dx in-H_2O/ft
1	2.500	410	410	$16.8\ 10^4$	$16.8\ 10^4$	-0.0511	0.0009	-0.050
2	2.450	400	810	$32.4\ 10^4$	$65.6\ 10^4$	-0.0985	0.0033	-0.095
3	2.355	390	1200	$46.8\ 10^4$	$144.0\ 10^4$	-0.1422	0.0073	-0.135
4	2.220	380	1580	$60.0\ 10^4$	$249.5\ 10^4$	-0.1823	0.0127	-0.170
5	2.050	370	1950	$72.1\ 10^4$	$380.0\ 10^4$	-0.2190	0.0193	-0.200
6	1.850	355	2305	$81.8\ 10^4$	$531.0\ 10^4$	-0.2490	0.0269	-0.222
7	1.628	330	2635	$87.0\ 10^4$	$695.0\ 10^4$	-0.2645	0.0353	-0.229
8	1.399	290	2925	$84.8\ 10^4$	$855.0\ 10^4$	-0.2580	0.0434	-0.215
9	1.184	245	3170	$77.7\ 10^4$	$1004.0\ 10^4$	-0.2360	0.0510	-0.185
10	0.999	230	3400	---	---	---	---	---

Radial depth of shelled corn, 11 ft

Radius of ventilating duct, 1 ft

Length of ventilating duct, 100 ft

Required air intake along duct, 50 cfm per ft

Fan on suction.

The static pressure difference required to pull 50 cfm of air per foot of length of duct through an 11-foot radial depth of shelled corn can be determined as approximately 0.25 inches of water from Figure 2 in Hukill and Ives' (20) article. A more accurate computation, using the information on which Hukill and Ives based Figure 2, gives the static pressure difference as 0.232 inches of water. At the dead end of the duct a static pressure of -0.232 inches of water will be required to pull 50 cfm of air through the grain. Since the static pressure in the duct will increase negatively toward the fan, a variable restriction to air flow through the duct wall must be introduced to limit the air intake to 50 cfm per foot. The required variation in the percent of open area of the duct wall to provide the necessary restriction can be determined by using Henderson's (13) results after the static pressure along the length of the duct is computed.

The static pressure along the length of the duct can be predicted from Equation 46. When $qx = Q$ is substituted in Equation 46, it integrates into

$$h = -\frac{M_s}{2} q^2 x^2 - \frac{N}{3} q^2 x^3 + h_o. \qquad (48)$$

If it is assumed that $K_s = 1.70$ and $f = 0.05$, the coefficients on x^2 and x^3 in Equation 48 become

$$\frac{M_s}{2} q^2 = \frac{K_s q^2}{A^2 2g} = \frac{(1.70)(50)^2}{(1.57)^2 (4005)^2} = 0.000108$$

$$\frac{N}{3} q^2 = \frac{fq^2}{3A^2 D2g} = \frac{(0.05)(50)^2}{(3)(1.57)^2 (1.22)^* (4005)^2} = 0.000000865$$

and Equation 48 can be written as

$$h = -0.000108x^2 - 0.000000865 x^3 + h_o \qquad (48a)$$

in which h = static pressure, inches of water

x = length of duct from dead end, ft.

The computations of the static pressures at 11 points along the duct are summarized in Table 3.

The excess static pressure, in addition to the static pressure required to pull 50 cfm of air per foot of length through the grain, is given in Table 3 in the column headed $h-h_o$. This excess static pressure must be dissipated in pulling the air through the duct wall.

*For a noncircular duct the hydraulic diameter is used where the hydraulic diameter is equal to four times the cross-sectional area divided by the wetted perimeter of the section.

Table 3. Summary of computation of static pressures in duct for Example 2

x ft	x^2	x^3	$-0.000108x^2$	$-0.000000865x^3$	$h-h_o$ in-H_2O	h in-H_2O
1	1	1	-0.000	-0.000	-0.000	-0.232
10	100	1,000	-0.011	-0.001	-0.012	-0.244
20	400	8,000	-0.043	-0.007	-0.050	-0.282
30	900	27,000	-0.097	-0.023	-0.120	-0.352
40	1,600	64,000	-0.173	-0.055	-0.228	-0.460
50	2,500	125,000	-0.270	-0.108	-0.378	-0.610
60	3,600	216,000	-0.389	-0.187	-0.576	-0.808
70	4,900	343,000	-0.529	-0.297	-0.826	-1.058
80	6,400	512,000	-0.691	-0.443	-1.134	-1.366
90	8,100	729,000	-0.875	-0.630	-1.505	-1.737
100	10,000	1,000,000	-1.080	-0.865	-1.945	-2.177

The percent open area of a duct wall that will dissipate the excess static pressure can be computed from the following equation given by Henderson (13):

$$\left[\begin{matrix}\text{Equivalent depth}\\ \text{of corn}\end{matrix}\right] \left[\begin{matrix}\text{Wall opening}\\ \text{percent}\end{matrix}\right]^{1.55} = 7.40.$$

Henderson's equation expresses the resistance to air flow through a perforated sheet in terms of the equivalent depth of corn to give the same pressure drop as the perforated sheet. For this example the equivalent depth of corn to use in Henderson's equation is found by dividing the excess static pressure by the static pressure drop per foot depth of corn corresponding to the air flow in cfm per square foot based on the surface area of the duct in contact with the grain. The air flow in cfm per square foot based on the surface area of the duct is

$$\frac{50 \text{ cfm/ft}}{3.14 \text{ sq ft/ft}} = 15.9 \text{ cfm/sq ft}.$$

Shedd's (33) data show for shelled corn and an air flow of 15.9 cfm per square foot the static pressure drop is 0.13 inches of water per foot depth of grain. When the excess static pressure is divided by 0.13, the equivalent depth of corn to use in Henderson's equation

is obtained and the percent open area of the duct can be computed. The computed required percent of open area of the duct wall is given in the last column of Table 4. The percent of open area of the duct wall increases without limit as the dead end of the duct is approached since additional restriction to the air flow is not required at the dead end. However, in view of Henderson's work, it will be necessary to provide a maximum open area of only 20 percent. To simplify this example, radial flow was assumed and no attempt was made to account for any diversion from radial flow.

Table 4. Required percent of open area of duct wall for Example 2

x ft	$h-h_o$ in-H_2O	Equivalent depth of corn ft	$\frac{7.40}{\text{Equivalent depth of corn}}$	Duct wall opening, percent
1	-0.000	0.00	∞	∞
10	-0.012	0.09	82.10	17.20
20	-0.050	0.39	19.00	6.68
30	-0.120	0.92	8.04	3.84
40	-0.228	1.75	4.23	2.54
50	-0.378	2.91	2.54	1.83
60	-0.576	4.43	1.67	1.39
70	-0.826	6.36	1.16	1.10
80	-1.134	8.73	0.85	0.90
90	-1.505	11.58	0.64	0.75
100	-1.945	14.98	0.49	0.63

SUMMARY

The rate of static pressure change in a perforated duct can be expressed as

$$\frac{dh}{dx} = -K \frac{d}{dx}\left[\frac{V^2}{2g}\right] \pm \frac{f V^2}{D\, 2g} \quad . \tag{52}$$

The minus sign on the friction term applies to a combining flow system in which the static pressure change associated with the velocity change adds to the static pressure change associated with friction. The plus sign on the friction term applies to a dividing flow system in which the static pressure change associated with the velocity change tends to offset the static pressure change associated with friction.

The friction term as expressed in Equation 52 is known as the Darcy-Weisbach formula for head loss. For noncircular ducts the diameter, D, is replaced by the hydraulic diameter.

The constant, K, applied to the rate of change of velocity head, can be determined experimentally for a given duct configuration. Theoretically, the value of K will be the same for both combining and dividing flow systems; however, the results of this study indicated the value of K for a dividing flow system can be expected to be less than the value of K for a combining flow system. The values

determined for the 5-inch diameter perforated test duct used in this study were:

Combining flow (suction system), $K_s = 1.70$

Dividing flow (pressure system), $K_p = 1.50$.

Equation 52 can be integrated to express the static pressure in the duct as a function of the length of the duct and the static pressure at the dead end whenever the velocity, V, can be written as a function of the duct length. When grain is ventilated, it often is desirable to maintain uniform air intake or discharge along the length of the duct. If uniform air intake or discharge is maintained, the velocity, V, will vary linearly along the length of the duct; and this relationship can be substituted in Equation 52. After the static pressure for uniform air distribution has been predicted, an auxiliary calibration is required to relate the static pressure in the duct to the air intake or discharge through the duct wall and the grain. This calibration is used to determine the required variation in the percent of open area of the duct to produce a uniform air intake or discharge along the length of the duct.

If the velocity distribution is unknown, Equation 52 can be solved by a numerical point-by-point procedure to determine the static pressure and air distribution. The numerical solution also requires an auxiliary calibration to relate the static pressure in the duct to the air intake or discharge.

CONCLUSIONS

1. The rate of static pressure change in a perforated grain ventilating duct can be expressed as a constant times the rate of velocity head change plus the rate of friction head change.

2. The value of the constant applied to the rate of velocity head change will approach a value of two for combining flow.

3. The value of the constant applied to the rate of velocity head change for dividing flow will be slightly less than the value applied to combining flow.

4. An equation of the form $dh/dx = -MqQ \pm N\Omega^2$ and information to relate static pressure in the duct to the air intake or discharge through the duct wall and through the grain the duct serves can be used to compute the percentage of openings required for a selected air distribution.

5. In a suction grain ventilating system (combining flow) the static pressure in the duct will increase negatively from the dead end to the fan end.

6. The relative value of the static pressure regain and duct friction loss will determine whether the static pressure in the duct for a pressure grain ventilating system (dividing flow) will decrease, increase, or remain constant from the dead end to the fan end.

LITERATURE CITED

1. Allen, John and Albinson, Brian. An investigation of the manifold problem for incompressible fluids with special reference to the use of manifolds for canal locks. Institution of Civil Engineers Proceedings. 4, no. 1: 114-138. Apr. 1955.

2. Carrier, Willis H., Cherne, Realto E., and Grant, Walter A. Modern air-conditioning, heating and ventilating. 2nd ed. New York, N. Y., Pitman Publishing Corporation. 1950.

3. Dow, Willard M. The uniform distribution of a fluid flowing through a perforated pipe. Journal of Applied Mechanics. 17: 431-438. Dec. 1950. In American Society of Mechanical Engineers Transactions. Vol. 72. 1950.

4. Edwards, F. W. Uniformly tapped pipes. [Letter]. Engineering News-Record. 126: 78. 1941.

5. Ellms, J. W. Design of perforated pipe strainer system. Journal of the American Water Works Association. 18: 664-674. 1927.

6. Enger, M. L. and Levy, M. I. Pressures in manifold pipes. Journal of the American Water Works Association. 21: 659-667. 1929.

7. Favre, Henry. Sur les lois régissant le mouvement des fluides dans les conduites en charge avec adduction latérale. Revue Universelle des Mines. 13: 502-512. 1937.

8. Gilman, S. F. Pressure losses of divided-flow fittings. American Society of Heating and Air-Conditioning Engineers Transactions. 61, no. 1538: 281-296. 1955.

9. _____. Pressure losses of divided-flow fittings. Heating, Piping and Air Conditioning. 27, no. 4: 141-147. 1955.

10. Gilman, Stanley Francis. Flow analysis of air duct systems. Unpublished Ph. D. Thesis. Urbana, Illinois, University of Illinois Library. 1953.

11. Gladding, R. D. Loss-of-head determination in uniformly tapped pipes. Engineering News-Record. 125: 697. 1940.

12. Hall, Carl W. Drying farm crops. Reynoldsburg, Ohio, Agricultural Consulting Associates, Inc. 1957.

13. Henderson, S. Milton. Resistance of shelled corn and bin walls to air flow. Agricultural Engineering. 24: 367-369, 374. 1943.

14. Holdsworth, J. F., Pritchard, F. W., and Walton, W. H. Fluid flow in ducts with a uniformly distributed leakage. British Journal of Applied Physics. 2: 321-324. Nov. 1951.

15. Holman, Leo E., comp. Aeration of grain in commercial storages. United States Department of Agriculture. Marketing Research Report No. 178. Sept. 1957.

16. Horlock, J. H. An investigation of the flow in manifolds with open and closed ends. Journal of the Royal Aeronautical Society. 60: 749-753. 1956.

17. Howland, W. E. Design of perforated pipe for uniformity of discharge. Third Midwestern Conference on Fluid Mechanics Proceedings. 1953: 687-701. 1953.

18. _____ . Gain in head at take-offs. Journal of the New England Water Works Association. 49, no. 1: 14. 1935.

19. _____ . Uniformly tapped pipes. [Letter]. Engineering News-Record. 126: 79. 1941.

20. Hukill, W. V. and Ives, N. C. Radial air flow resistance of grain. Agricultural Engineering. 36: 332-335. 1955.

21. Johnson, Howard K. Cooling stored grain by aeration. Agricultural Engineering. 38: 238-241, 244-246. 1957.

22. Keller, J.D., Jr. The manifold problem. Journal of Applied Mechanics. 16: 77-85. March 1949. In American Society of Mechanical Engineers Transactions. Vol. 71. 1949.

23. Kunz, Jakob. Jets from manifold tubes. American Society of Mechanical Engineers Transactions. 53: 181-186. 1931.

24. Madison, Richard D., ed. Fan engineering. 5th ed. Buffalo, New York, Buffalo Forge Company. 1949.

25. Malishevsky, N. Pressure head in perforated pipes. Journal of the American Water Works Association. 27: 413-418. 1935.

26. Malishewsky, N. Discussion, the hydraulics of filter underdrains. Journal of the American Water Works Association. 20: 416-418. 1928.

27. McNown, John S. Mechanics of manifold flow. American Society of Civil Engineers Proceedings. 79, no. 258: 1-22. Aug. 1953.

28. National Association of Fan Manufacturers, Inc. NAFM Bulletin No. 110, 2nd ed. Detroit, Michigan, Author. 1952.

29. Oakey, John A. Hydraulic losses in short tubes determined by experiments. Engineering News-Record. 110: 717-718. 1933.

30. Rabe, F. W. Aeration of grain in vertical bins. Agricultural Engineering. 39: 98-103. 1958.

31. Robinson, R. N., Hukill, W. V., and Foster, G. H. Mechanical ventilation of stored grain. Agricultural Engineering. 32: 606-608. 1951.

32. Shedd, C. K. Measuring air flow with perforated metal sheet. Agricultural Engineering. 35: 420. 1954.

33. _____ . Resistance of grains and seeds to air flow. Agricultural Engineering. 34: 616-619. 1953.

34. Soucek, Edward, and Zelnick, E. W. Lock manifold experiments. American Society of Civil Engineers Transactions. 110: 1357-1378. 1945.

35. Stevens, J. C. Theoretical energy losses in intersecting pipes. Engineering News-Record. 97: 140-141. 1926.

36. Theimer, Otto F. Ventilation of grain storages. Agricultural Engineering. 32: 106, 108, 110. 1951.

ACKNOWLEDGMENTS

Sincere appreciation is expressed for the counsel and guidance given by Professor William V. Hukill and Doctor Glenn Murphy during this study. Gratitude is expressed for the helpful suggestions of Professor Hobart Beresford, Head of the Department of Agricultural Engineering; and acknowledgment is made to the Department of Agricultural Engineering and to the United States Department of Agriculture for the use of their facilities.

Appreciation also is expressed for the encouragement offered by Mr. Tappan Collins and Mr. Earl D. Anderson; and acknowledgment is made to the Stran-Steel Corporation, whose financial assistance made this study possible.

APPENDIX A: METHOD OF CALIBRATING PERFORATED METAL SHEETS USED FOR AIR FLOW MEASUREMENT

The perforated metal sheets used for air flow measurements were calibrated in place by making a standard pitot tube traverse in the test duct. Since it was not possible to make a ten-point traverse with a standard 5/16-inch diameter pitot tube in the 5-inch diameter duct, a six-point traverse, as outlined by Madison (24, p. 108), was used. Each traverse consisted of 12 readings, six readings on a horizontal diameter and six on a vertical diameter. The air flow in cfm was calculated according to the procedure and formulae given in the NAFM Bulletin No. 10 (28).

Shedd (32) suggested it is best to provide for the air to enter the perforations from the square-edge side. Since the perforated metal sheets in the collector units on the duct (Fig. 9) could be reversed easily, the sheets on these units were arranged to allow the air to enter the square-edge side under both suction and pressure conditions. The larger perforated metal sheet used to measure air flow at the end of the duct could not be reversed conveniently. Consequently, when the duct was under pressure, the air entered the rounded-edge side of the perforations in this sheet. The calibration curves are shown in Figure 15.

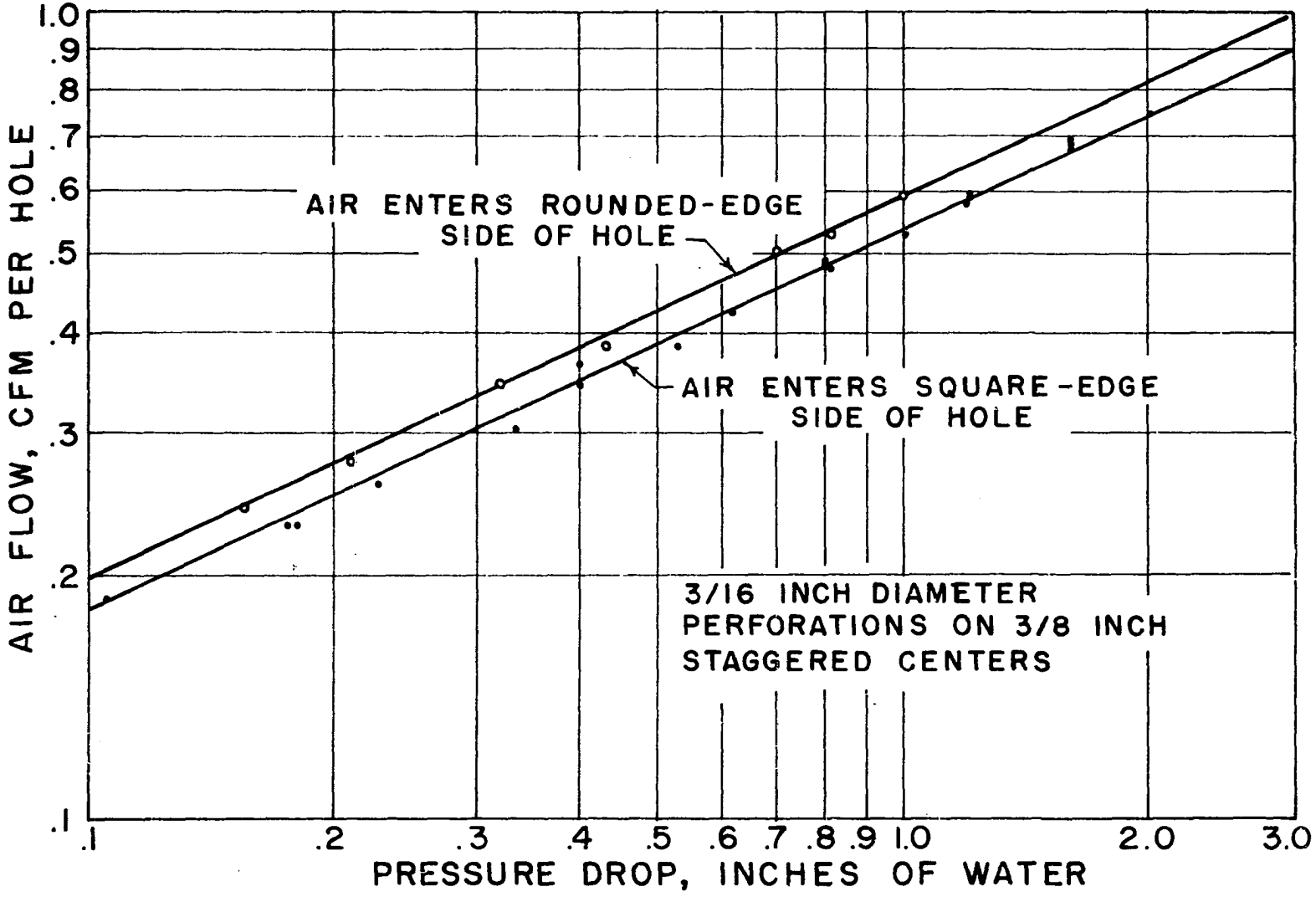

Fig. 15. Calibration chart for perforated metal sheet

APPENDIX B: DETERMINATION OF THE FRICTION HEAD LOSS FOR THE TEST DUCT

The friction loss for the test duct was determined experimentally by sealing the outside surface of the duct with masking tape and observing the static pressure drop in the duct for various air flow rates. A plot of the data (Fig. 16) indicated for practical purposes the friction loss was proportional to the square of the velocity or flow rate. The friction curve therefore was drawn on the basis of this relationship. The line was extended to low flow rates on the basis the friction factor, f, in the Darcy-Weisbach equation

$$h_f = f \frac{L}{D} \frac{V^2}{2g}$$

remains constant.

Although the friction factor does vary in the region below complete turbulence as shown by the Moody or Stanton diagram found in textbooks on fluid mechanics, the assumption of constancy will suffice. Since the friction factor for the test duct was equal to approximately 0.025, any marked change in the friction factor would occur below a Reynolds number of about 50,000. A Reynolds number of 50,000 corresponds to a velocity of approximately 1200 ft/min (164 cfm) in the 5-inch diameter test duct. Consequently, any appreciable deviation from the straight line indicated in Fig. 16 would occur below 164 cfm. Although

friction losses for short lengths of duct with low flow rates are of a negligible order, the increase in the friction factor as the flow approaches the critical zone would cause a corresponding increase in the friction loss.

Figure 16 was assumed to apply to the test duct when air was allowed to enter or leave the duct at selected points along its length.

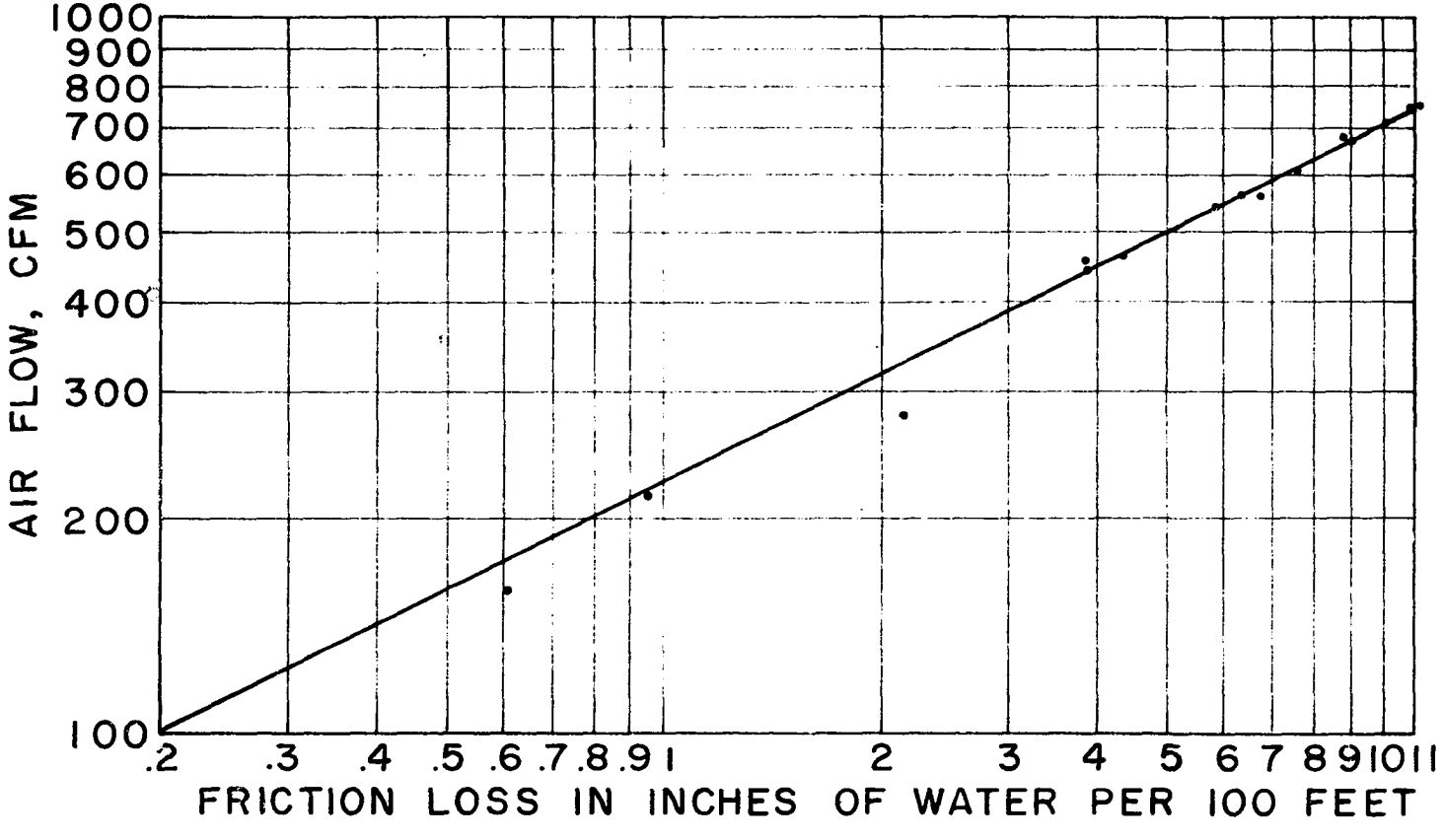

Fig. 16. Friction loss for 5-inch diameter perforated metal duct with no air flow through perforations

APPENDIX C: AIR FLOW CALIBRATION OF THE PERFORATIONS IN THE TEST DUCT WALL

A convenient method of varying the area of an opening in the test duct wall was to vary the number of circumferential rows of perforations left uncovered. Each circumferential row of perforations contained 123 perforations of 0.078-inch diameter. Hence, each row left uncovered provided an air entry or discharge area of approximately 0.588 square inches. For convenience the calibration curves (Figs. 17 and 18) were plotted in terms of the number of open circumferential rows of perforations.

It was necessary to select a point in the duct near the vicinity of the opening where a static pressure might be observed to which the rate of air entry or discharge could be related. A point on the center line of the duct 1 inch downstream from the downstream edge of the opening was selected.

The intake and discharge flow rates during the calibration tests were determined by use of the collector units previously described (Fig. 9). The static pressures plotted in Figures 17 and 18 were obtained by subtracting the collector unit static pressures from the static pressures observed in the duct at the point indicated. Figures 17 and 18 were used to determine the flow rate for openings not restricted by collector units.

In the literature reviewed, several investigators indicated the coefficient of discharge is a function of the velocity in the duct. Their results indicated a decrease in the coefficient of discharge with increase of flow rate in the main duct. However, it was not possible to detect any significant variation in the coefficient of discharge from the data for the test duct. The data (Figs. 17 and 18) indicated the intake and discharge flow rates conformed to the square law.

Soucek and Zelnick (34, p. 1399) indicated the coefficient of discharge can be shown to be a function of the flow ratio, q/Q, by performing the following successive transformations on the flow equation, $q = C_d\ a\sqrt{2gh}$:

$$C_d = \frac{q}{a\sqrt{2gh}} = \frac{qQ}{a\sqrt{2gh}\,Q} = \frac{qAV}{a\sqrt{2gh}\,Q} = \sqrt{\left(\frac{q}{Q}\right)^2 \left(\frac{A}{a}\right)^2 \frac{V^2}{2gh}}.$$

Since $\frac{V^2}{2gh}$ could be shown to be a function of the flow ratio, q/Q, in a manner similar to the way $\Delta h/V^2/2g$ is shown to be a function of q/Q (Fig. 10), the coefficient of discharge becomes a function of the flow ratio, q/Q.

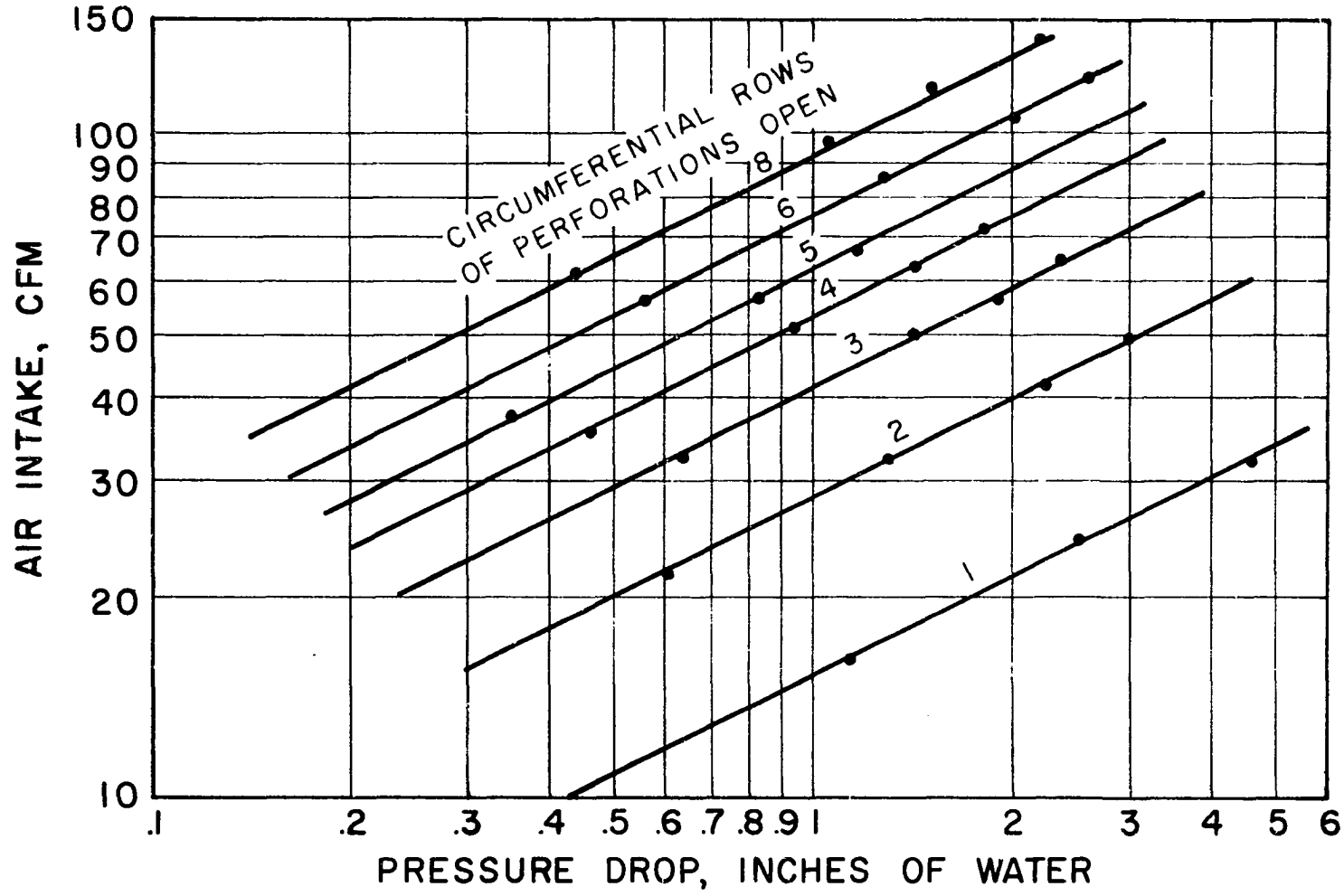

Fig. 17. Air intake calibration chart for 5-inch diameter perforated metal duct

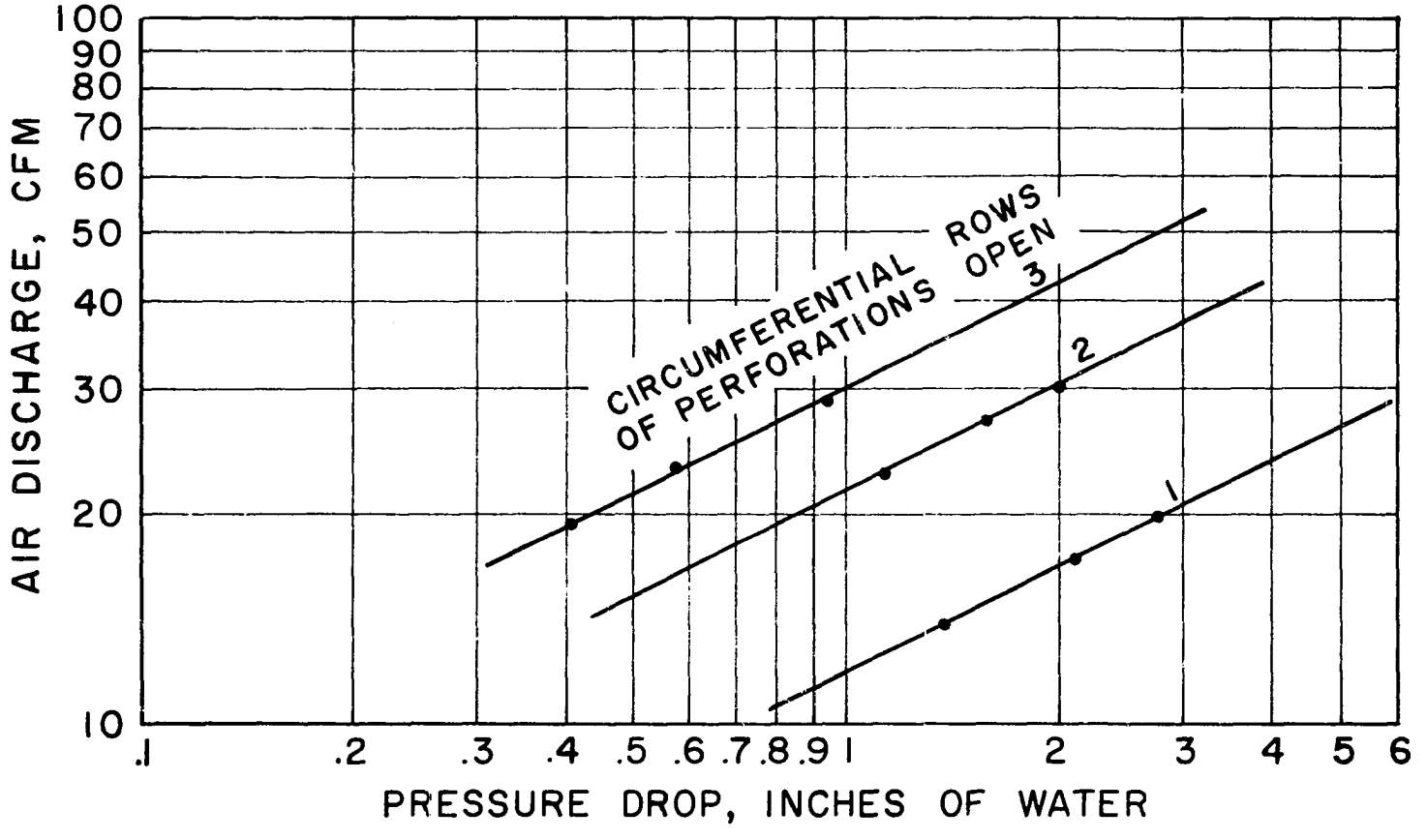

Fig. 18. Air discharge calibration chart for 5-inch diameter perforated metal duct

APPENDIX D: ORIGINAL AND CALCULATED DATA

Table 5. Original data for Figure 10

Test No. and position*	Static pressure drop across perforated sheet at the upstream end of the duct, in-H_2O	No. of holes open in perforated sheet at upstream end of duct	Static pressure drop across perforated sheet in collector unit, in-H_2O	No. of holes open in perforated sheet in collector unit	Static pressure drop along 3 ft of duct, Δh, in-H_2O
1 a	0.615	1,555	0.190	99	0.423
b			0.290	80	0.460
c			1.640	35	0.475
2 a	0.226	1,555	0.540	60	0.210
b			0.290	80	0.232
c			1.540	36	0.240
3 a	0.334	510	2.100	31	0.065
b			1.540	36	0.073
c			2.820	27	0.070
4 a	0.190	100	2.110	31	0.016
b			1.540	36	0.017
c			2.810	27	0.011
5 a	0.310	790	2.080	31	0.102
b			1.540	36	0.120
c			2.850	27	0.120

*The letters a, b, and c refer to consecutive positions from the upstream end of the duct.

Table 5 (Continued)

Test No. and position*	Static pressure drop across perforated sheet at the upstream end of the duct, in-H_2O	No. of holes open in perforated sheet at upstream end of duct	Static pressure drop across perforated sheet in collector unit, in-H_2O	No. of holes open in perforated sheet in collector unit	Static pressure drop along 3 ft of duct, Δh, in-H_2O
6 a	0.688	1,555	2.860	11	0.353
b			3.040	11	0.389
c			3.630	10	0.400
7 a	0.350	1,555	3.070	11	0.210
b			3.100	11	0.228
c			3.600	10	0.230
8 a	0.495	790	3.200	11	0.094
b			3.160	11	0.101
c			3.550	10	0.100
9 a	0.290	340	3.050	11	0.023
b			2.950	11	0.025
c			3.200	11	0.026
10 a	0.290	340	3.640	5	0.020
b			3.650	5	0.020
c			3.670	5	0.018
11 a	0.715	1,555	3.350	5	0.326
b			3.600	5	0.355
c			4.000	5	0.362

Table 5 (Continued)

Test No. and position*	Static pressure drop across perforated sheet at the upstream end of the duct, in-H_2O	No. of holes open in perforated sheet at upstream end of duct	Static pressure drop across perforated sheet in collector unit, in-H_2O	No. of holes open in perforated sheet in collector unit	Static pressure drop along 3 ft of duct, Δh, in-H_2O
12 a	0.730	1,555	3.450	4	0.324
b			3.750	4	0.353
c			3.950	6	0.392
13 a	0.350	1,555	3.450	4	0.175
b			3.600	4	0.190
c			3.640	6	0.212
14 a	0.920	790	3.750	4	0.130
b			3.840	4	0.135
c			3.840	6	0.150
15 a	0.473	790	3.200	4	0.070
b			3.250	4	0.075
c			3.200	6	0.080
16 a	0.660	1,555	0.195	100	0.456
b			1.030	40	0.478
c			3.200	16	0.450
17 a	0.310	1,555	0.250	100	0.290
b			1.230	40	0.306
c			3.750	16	0.275

Table 5 (Continued)

Test No. and position*	Static pressure drop across perforated sheet at the upstream end of the duct, in-H_2O	No. of holes open in perforated sheet at upstream end of duct	Static pressure drop across perforated sheet in collector unit, in-H_2O	No. of holes open in perforated sheet in collector unit	Static pressure drop along 3 ft of duct, Δh, in-H_2O
18 a	0.663	1,555	0.505	32	0.356
b			1.020	40	0.468
c			3.150	16	0.435
19 a	0.540	1,555	0.470	32	0.302
b			0.950	40	0.392
c			2.900	16	0.365
20 a	0.420	1,555	0.475	32	0.250
b			0.950	40	0.328
c			2.900	16	0.300
21 a	0.302	1,555	0.480	32	0.195
b			0.940	40	0.261
c			2.850	16	0.236
22 a	0.382	1,555	1.340	300	1.610
b			1.000	40	0.462
c			3.100	16	0.470
23 a	0.145	1,555	1.870	300	1.290
b			1.160	40	0.341
c			3.500	16	0.323

Table 5 (Continued)

Test No. and position*	Static pressure drop across perforated sheet at the upstream end of the duct, in-H_2O	No. of holes open in perforated sheet at upstream end of duct	Static pressure drop across perforated sheet in collector unit, in-H_2O	No. of holes open in perforated sheet in collector unit	Static pressure drop along 3 ft of duct, Δh, in-H_2O
24 a	0.445	510	2.300	300	0.945
b			1.260	40	0.247
c			3.840	16	0.221
25 a	0.470	340	1.320	300	0.515
b			0.695	40	0.131
c			2.160	16	0.117
26 a	0.240	340	0.630	300	0.270
b			0.350	40	0.068
c			1.120	16	0.060

Table 6. Calculated data for plotting Figure 10

Test No. and position*	q cfm	Q_u cfm	Q_d cfm	$V_d^2/2g$ in-H_2O	Δh corrected for duct friction in-H_2O	$\frac{\Delta h \text{ corrected}}{V_d^2/2g}$	q/Q_d
1 a	24.2	655.0	679.2	1.5480	0.162	0.1050	0.0357
b	23.9	679.2	703.1	1.6570	0.180	0.1080	0.0340
c	24.0	703.1	727.1	1.7700	0.175	0.0990	0.0330
2 a	24.0	407.0	431.0	0.6230	0.106	0.1700	0.0557
b	23.9	431.0	454.9	0.6950	0.116	0.1670	0.0526
c	24.0	454.9	478.9	0.7690	0.111	0.1440	0.0501
3 a	24.0	161.0	185.0	0.1150	0.047	0.4080	0.1300
b	24.0	185.0	209.0	0.1460	0.050	0.3420	0.1150
c	24.1	209.0	233.1	0.1820	0.041	0.2250	0.1035
4 a	24.0	24.1	48.1	0.0078	0.015	1.9350	0.5000
b	24.0	48.1	72.1	0.0174	0.015	0.8620	0.3330
c	24.0	72.1	96.1	0.0310	0.007	0.2260	0.2500
5 a	23.9	240.0	263.9	0.2340	0.064	0.2740	0.0906
b	24.0	263.9	287.9	0.2780	0.075	0.2700	0.0836
c	24.2	287.9	312.1	0.3270	0.067	0.2050	0.0775

*The letters a, b, and c refer to consecutive positions from the upstream end of the duct.

Table 6 (Continued)

Test No. and position*	q cfm	Q_u cfm	Q_d cfm	$V_d^2/2g$ in-H_2O	Δh corrected for duct friction in-H_2O	$\frac{\Delta h \text{ corrected}}{V_d^2/2g}$	q/Q_d
6 a	9.9	690.0	699.9	1.6400	0.070	0.0427	0.0140
b	10.2	699.9	710.1	1.6900	0.099	0.0585	0.0144
c	10.1	710.1	720.2	1.7400	0.101	0.0580	0.0140
7 a	10.2	500.0	510.2	0.8720	0.059	0.0676	0.0200
b	10.3	510.2	520.5	0.9090	0.071	0.0780	0.0198
c	10.0	520.5	530.5	0.9450	0.067	0.0709	0.0189
8 a	10.4	300.0	310.4	0.3230	0.039	0.1207	0.0336
b	10.4	310.4	320.8	0.3450	0.042	0.1217	0.0324
c	10.0	320.8	330.8	0.3670	0.037	0.1010	0.0302
9 a	10.2	100.3	110.5	0.0409	0.016	0.3910	0.0905
b	10.0	110.5	120.5	0.0486	0.017	0.3500	0.0830
c	10.4	120.5	130.9	0.0574	0.017	0.2960	0.0795
10 a	5.1	100.3	105.4	0.0372	0.014	0.3760	0.0483
b	5.1	105.4	110.5	0.0410	0.013	0.3170	0.0461
c	5.1	110.5	115.6	0.0446	0.010	0.2240	0.0441
11 a	4.9	705.0	709.9	1.6900	0.032	0.0189	0.0069
b	5.1	709.9	715.0	1.7150	0.057	0.0332	0.0071
c	5.3	715.0	720.3	1.7400	0.060	0.0345	0.0074

Table 6 (Continued)

Test No. and position*	q cfm	Q_u cfm	Q_d cfm	$V_d^2/2g$ in-H_2O	Δh corrected for duct friction in-H_2O	$\frac{\Delta h \text{ corrected}}{V_d^2/2g}$	q/Q_d
12 a	3.9	711.0	714.9	1.7150	0.026	0.0152	0.0055
b	4.1	714.9	719.0	1.7350	0.052	0.0300	0.0057
c	6.3	719.0	725.3	1.7650	0.087	0.0492	0.0087
13 a	3.9	501.0	504.9	0.8550	0.026	0.0304	0.0077
b	4.0	504.9	508.9	0.8680	0.038	0.0437	0.0078
c	6.1	508.9	515.0	0.8900	0.057	0.0640	0.0118
14 a	4.1	403.0	407.1	0.5550	0.033	0.0595	0.0101
b	4.1	407.1	411.2	0.5670	0.036	0.0635	0.0100
c	6.2	411.2	417.4	0.5850	0.049	0.0838	0.0148
15 a	3.8	294.0	297.8	0.2970	0.018	0.0606	0.0128
b	3.8	297.8	301.6	0.3050	0.022	0.0721	0.0126
c	5.7	301.6	307.3	0.3170	0.025	0.0790	0.0186
16 a	24.7	677.0	701.7	1.6500	0.177	0.1072	0.0352
b	22.0	701.7	723.7	1.7560	0.179	0.1020	0.0304
c	15.2	723.7	738.9	1.8330	0.136	0.0742	0.0206
17 a	27.8	473.0	500.8	0.8410	0.150	0.1782	0.0556
b	24.0	500.8	524.8	0.9230	0.151	0.1638	0.0458
c	16.4	524.8	541.2	0.9830	0.108	0.1100	0.0304

Table 6 (Continued)

Test No. and position*	q cfm	Q_u cfm	Q_d cfm	$V_d^2/2g$ in-H_2O	Δh corrected for duct friction in-H_2O	$\frac{\Delta h \text{ corrected}}{V_d^2/2g}$	q/Q_d
18 a	12.5	680.0	692.5	1.6090	0.081	0.0503	0.0181
b	21.8	692.5	714.3	1.7120	0.178	0.1038	0.0305
c	15.0	714.3	729.3	1.7850	0.129	0.0723	0.0206
19 a	12.1	616.0	628.1	1.3230	0.076	0.0574	0.0193
b	21.1	628.1	649.2	1.4150	0.153	0.1080	0.0325
c	14.5	649.2	663.7	1.4450	0.113	0.0782	0.0218
20 a	12.1	546.0	558.1	1.0450	0.071	0.0680	0.0216
b	21.1	558.1	579.2	1.1240	0.138	0.1226	0.0364
c	14.5	579.2	593.7	1.1830	0.098	0.0828	0.0244
21 a	12.2	467.0	479.2	0.7700	0.063	0.0820	0.0253
b	21.0	479.2	500.2	0.8400	0.120	0.1430	0.0420
c	14.4	500.2	514.6	0.8890	0.084	0.0945	0.0280
22 a	186.9	522.0	708.9	1.6870	1.382	0.8200	0.2630
b	21.7	708.9	730.6	1.7900	0.158	0.0883	0.0297
c	15.0	730.6	745.6	1.8650	0.150	0.0805	0.0201
23 a	219.0	330.0	549.0	1.0100	1.169	1.1570	0.3990
b	23.2	549.0	572.2	1.1000	0.156	0.1417	0.0405
c	15.8	572.2	588.0	1.1600	0.125	0.1077	0.0268

Table 6 (Continued)

Test No. and position*	q cfm	Q_u cfm	Q_d cfm	$V_d^2/2g$ in-H_2O	Δh corrected for duct friction in-H_2O	$\frac{\Delta h \text{ corrected}}{V_d^2/2g}$	q/Q_d
24 a	243.0	184.0	427.0	0.6110	0.881	1.4410	0.5680
b	24.1	427.0	451.1	0.6830	0.133	0.1946	0.0534
c	16.5	451.1	467.6	0.7330	0.097	0.1320	0.0352
25 a	185.4	126.0	311.4	0.3250	0.482	1.4820	0.5950
b	18.2	311.4	329.6	0.3640	0.070	0.1920	0.0552
c	12.5	329.6	342.1	0.3920	0.050	0.1275	0.0365
26 a	130.2	64.6	194.8	0.1272	0.258	2.0300	0.6680
b	13.1	194.8	207.9	0.1465	0.044	0.3010	0.0630
c	9.1	207.9	217.0	0.1580	0.033	0.2090	0.0419

Table 7. Computed static pressures, observed static pressures, and air intake plotted in Figure 11

Duct Length, ft	h* in-H_2O	q cfm/opening	Q cfm	MqQ**	NQ^2***	dh/dx in-H_2O/1/2 ft	h/1.0/0.77 in-H_2O	h(Obs.) in-H_2O	q(Obs.) cfm/opening
0.0	-1.0000	28.60	28.60	0.0093	0.0001	-0.0094	-0.770	-0.770	24.0
0.5	-1.0094	28.73	57.33	0.0188	0.0003	-0.0191	-0.776	-0.770	25.0
1.0	-1.0285	29.00	86.33	0.0286	0.0007	-0.0293	-0.791	-0.790	25.3
1.5	-1.0578	29.42	115.75	0.0388	0.0013	-0.0401	-0.814	-0.825	25.9
2.0	-1.0979	29.97	145.72	0.0498	0.0021	-0.0519	-0.845	-0.855	26.5

*Static pressure of -1.0 in-H_2O was arbitrarily chosen as a beginning point for the computations. When the static pressures in Column 2 are divided by the ratio of 1.0 to the observed static pressure at the dead end, the values of computed static pressures (Column 8) corresponding to a beginning point static pressure equal to the observed dead end static pressure are obtained.

**$M = (11.4)\ 10^{-6}$.

***$N = (0.0983)\ 10^{-6}$.

Table 7 (Continued)

Duct Length, ft	h* in-H_2O	q cfm/opening	Q cfm	MqQ**	NQ^2***	$\frac{dh}{dx}$ in-H_2O/1/2 ft	$\frac{h}{1.0/0.77}$ in-H_2O	h(Obs.) in-H_2O	q(Obs.) cfm/opening
2.5	-1.1498	30.67	176.39	0.0617	0.0030	-0.0647	-0.884	-0.910	27.2
3.0	-1.2145	31.52	207.91	0.0747	0.0043	-0.0790	-0.935	-0.980	28.3
3.5	-1.2935	32.53	240.44	0.0892	0.0057	-0.0949	-0.995	-1.070	29.5
4.0	-1.3884	33.70	274.14	0.1053	0.0074	-0.1127	-1.068	-1.160	30.7
4.5	-1.5011	35.04	309.18	0.1235	0.0094	-0.1329	-1.156	-1.240	31.8
5.0	-1.6340	36.56	345.74	0.1441	0.0118	-0.1559	-1.260	-1.340	33.0
5.5	-1.7899	38.26	384.00	0.1675	0.0145	-0.1820	-1.377	-1.450	34.4
6.0	-1.9719	40.16	424.16	0.1942	0.0177	-0.2119	-1.519	-1.620	36.3
6.5	-2.1838	42.27	466.43	0.2248	0.0214	-0.2462	-1.680	-1.800	38.3
7.0	-2.4300	44.58	511.01	0.2597	0.0257	-0.2854	-1.872	-2.040	40.8
7.5	-2.7154	47.13	558.14	0.2999	0.0306	-0.3305	-2.092	-2.300	43.2
8.0	-3.0459	49.91	608.05	0.3460	0.0363	-0.3823	-2.345	-2.560	45.7
8.5	-3.4282	52.95	661.00	0.3990	0.0429	-0.4419	-2.640	-2.920	48.8
9.0	-3.8701	56.26	717.26	0.4600	0.0506	-0.5106	-2.980	-3.430	53.0
9.5	-4.3807	59.86	777.12	0.5303	0.0594	-0.5897	-3.380	-3.900	56.5

Table 8. Computed static pressures, observed static pressures, and air intake plotted in Figure 12

Duct Length, ft	q cfm/opening	x 1/2 ft	$\frac{M}{2} q^2 x^{2*}$	$\frac{N}{3} q^2 x^{3**}$	$h-h_o$*** in-H_2O	h in-H_2O	h(Obs.) in-H_2O	q(Obs.) cfm/opening	Circumferential rows of perforations open per opening
0.0	30.0	1	0.005	0.000	-0.005	-0.205	-0.130	24.0	5.25
0.5	30.0	2	0.021	0.000	-0.021	-0.221	-0.180	27.0	5.00
1.0	30.0	3	0.046	0.001	-0.047	-0.247	-0.215	28.0	4.75
1.5	30.0	4	0.082	0.002	-0.084	-0.284	-0.250	28.4	4.33
2.0	30.0	5	0.128	0.004	-0.132	-0.332	-0.300	28.5	3.88
2.5	30.0	6	0.185	0.006	-0.191	-0.391	-0.355	28.5	3.50
3.0	30.0	7	0.251	0.010	-0.261	-0.461	-0.440	29.5	3.25
3.5	30.0	8	0.328	0.015	-0.343	-0.543	-0.520	29.5	2.92
4.0	30.0	9	0.416	0.022	-0.438	-0.638	-0.595	29.0	2.63
4.5	30.0	10	0.513	0.030	-0.543	-0.743	-0.710	29.5	2.50

*$M = (11.4)\ 10^{-6}$.

**$N = (0.0983)\ 10^{-6}$.

***$h_o = -0.200$ in-H_2O.

Table 8 (Continued)

Duct Length, ft	q cfm / opening	x 1/2 ft	$\frac{M}{2}q^2x^{2*}$	$\frac{N}{3}q^2x^{3**}$	$h-h_o^{***}$ in-H_2O	h in-H_2O	h(Obs.) in-H_2O	q(Obs.) cfm / opening	Circumferential rows of perforations open per opening
5.0	30.0	11	0.621	0.039	-0.660	-0.860	-0.820	29.4	2.33
5.5	30.0	12	0.738	0.051	-0.789	-0.989	-0.940	29.5	2.17
6.0	30.0	13	0.867	0.062	-0.929	-1.129	-1.080	29.4	2.00
6.5	30.0	14	1.005	0.081	-1.086	-1.286	-1.240	29.5	1.88
7.0	30.0	15	1.153	0.100	-1.253	-1.453	-1.420	29.7	1.78
7.5	30.0	16	1.314	0.121	-1.435	-1.635	-1.570	29.5	1.67
8.0	30.0	17	1.485	0.145	-1.630	-1.830	-1.730	29.2	1.60
8.5	30.0	18	1.665	0.172	-1.837	-2.037	-1.990	29.8	1.50
9.0	30.0	19	1.855	0.203	-2.058	-2.258	-2.280	30.0	1.45
9.5	30.0	20	2.050	0.236	-2.286	-2.486	-2.500	30.0	1.38

Table 9. Computed static pressures, observed static pressures, and air discharge plotted in Figure 13

Duct Length, ft	h* in-H_2O	q cfm / opening	Q cfm	MqQ**	NQ^2***	$\frac{dh}{dx}$ in-H_2O / 1/2 ft	$\frac{h}{1.0/3.83}$ in-H_2O	h(Obs.) in-H_2O	q(Obs.) cfm / opening
0.0	1.0000	21.20	21.20	0.0045	0.0000	-0.0045	3.830	3.83	41.4
0.5	0.9955	21.15	42.35	0.0090	0.0002	-0.0088	3.813	3.80	41.2
1.0	0.9867	21.06	63.41	0.0134	0.0004	-0.0130	3.779	3.78	41.1
1.5	0.9737	20.92	84.33	0.0176	0.0007	-0.0169	3.729	3.70	40.7
2.0	0.9568	20.74	105.07	0.0218	0.0011	-0.0207	3.665	3.65	40.3
2.5	0.9361	20.51	125.58	0.0258	0.0016	-0.0242	3.585	3.55	39.9
3.0	0.9119	20.24	145.82	0.0295	0.0021	-0.0274	3.493	3.45	39.2
3.5	0.8845	19.94	165.76	0.0331	0.0027	-0.0304	3.388	3.35	38.7
4.0	0.8541	19.59	185.35	0.0363	0.0034	-0.0329	3.271	3.24	38.1
4.5	0.8212	19.21	204.56	0.0393	0.0039	-0.0354	3.145	3.10	37.2

*A static pressure of 1.0 in-H_2O was arbitrarily chosen as a beginning point for the computations. When the static pressures in Column 2 are divided by the ratio of 1.0 to the observed static pressure at the dead end, the values of computed static pressures (Column 8) corresponding to a beginning point static pressure equal to the observed dead end static pressure are obtained.

**$M = (10.0)\ 10^{-6}$.

***$N = (0.0983)\ 10^{-6}$.

Table 9 (Continued)

Duct Length, ft	h* in-H_2O	q cfm / opening	Q cfm	MqQ**	NQ^2***	dh/dx in-H_2O / 1/2 ft	h / 1.0/3.83 in-H_2O	h(Obs.) in-H_2O	q(Obs.) cfm / opening
5.0	0.7858	18.79	223.35	0.0420	0.0049	-0.0371	3.010	2.99	36.6
5.5	0.7487	18.34	241.69	0.0443	0.0057	-0.0386	2.868	2.83	35.5
6.0	0.7101	17.87	259.56	0.0464	0.0066	-0.0398	2.720	2.70	34.7
6.5	0.6703	17.36	276.92	0.0481	0.0075	-0.0405	2.567	2.55	33.7
7.0	0.6298	16.82	293.74	0.0494	0.0085	-0.0409	2.412	2.40	32.7
7.5	0.5889	16.27	310.01	0.0504	0.0094	-0.0410	2.255	2.22	31.4
8.0	0.5479	15.69	325.70	0.0511	0.0104	-0.0407	2.098	2.07	30.2
8.5	0.5072	15.10	340.80	0.0515	0.0114	-0.0401	1.943	1.93	29.4
9.0	0.4672	14.49	355.29	0.0515	0.0124	-0.0391	1.789	1.70	27.6
9.5	0.4281	13.87	369.16	0.0512	0.0134	-0.0378	1.640	1.57	26.5

Table 10. Computed static pressures, observed static pressures, and air intake plotted in Figure 14

Duct Length, ft	q cfm/opening	x 1/2 ft	$\frac{M}{2} q^2x^2$*	$\frac{N}{3} q^2x^3$**	$h-h_o$*** in-H_2O	h in-H_2O	h(Obs.) in-H_2O	q(Obs.) cfm/opening	Circumferential rows of perforations open per opening
0.0	30.0	1	0.005	0.000	-0.005	2.995	3.00	30.0	1.66
0.5	30.0	2	0.018	0.000	-0.018	2.982	2.99	30.0	1.66
1.0	30.0	3	0.041	0.001	-0.040	2.960	2.96	30.0	1.67
1.5	30.0	4	0.072	0.002	-0.070	2.930	2.92	30.0	1.68
2.0	30.0	5	0.113	0.004	-0.109	2.891	2.90	30.0	1.69
2.5	30.0	6	0.162	0.006	-0.156	2.844	2.85	30.0	1.70
3.0	30.0	7	0.220	0.010	-0.210	2.790	2.79	30.0	1.71
3.5	30.0	8	0.288	0.015	-0.273	2.727	2.71	30.0	1.73
4.0	30.0	9	0.365	0.022	-0.343	2.657	2.65	30.0	1.75
4.5	30.0	10	0.450	0.030	-0.420	2.580	2.58	30.0	1.77

*$M = (10.0)\ 10^{-6}$.

**$N = (0.0983)\ 10^{-6}$.

***$h_o = 3.000$ in-H_2O.

Table 10 (Continued)

Duct Length ft	q $\frac{\text{cfm}}{\text{opening}}$	x 1/2 ft	$\frac{M}{2} q^2x^2$*	$\frac{N}{3} q^2x^3$**	$h-h_o$*** in-H_2O	h in-H_2O	h(Obs.) in-H_2O	q(Obs.) $\frac{\text{cfm}}{\text{opening}}$	Circumferential rows of perforations open per opening
5.0	30.0	11	0.545	0.040	-0.505	2.495	2.49	30.0	1.79
5.5	30.0	12	0.648	0.051	-0.597	2.403	2.39	30.0	1.82
6.0	30.0	13	0.760	0.062	-0.698	2.302	2.30	30.0	1.86
6.5	30.0	14	0.882	0.081	-0.801	2.199	2.18	30.0	1.93
7.0	30.0	15	1.012	0.100	-0.912	2.088	2.07	30.0	1.98
7.5	30.0	16	1.152	0.121	-1.031	1.969	1.96	30.0	2.04
8.0	30.0	17	1.301	0.145	-1.156	1.844	1.82	29.8	2.12
8.5	30.0	18	1.458	0.172	-1.286	1.714	1.67	29.6	2.24
9.0	30.0	19	1.624	0.203	-1.421	1.579	1.51	29.5	2.36
9.5	30.0	20	1.800	0.236	-1.564	1.436	1.35	29.0	2.48